Chapter 3

Geotechnical Design Considerations

Marshall Lew, Ph.D., G.E.
Corporate Consultant, Law/Crandall, a division of Law Engineering and Environmental Services, Inc. (A LAWGIBB Group Member), Los Angeles

Key words: Building Code, Earthquake Ground Motion, Fault Rupture, International Building Code, Landslides, Lateral Spreading, Liquefaction Analysis, Liquefaction Mitigation, Near-Source Effects, Response Spectra, Settlement, Site Effects, Soil-Structure Interaction, Soil Profiles, Tsunamis, Uniform Building Code.

Abstract: This chapter surveys the interactions between structural and geotechnical engineering in earthquake-resistant design. The effects of the local site conditions and geology are presented as applied in the Uniform Building Code and in the new International Building Code. Methods of characterizing the site conditions, as well as consideration of near-source effects, are discussed. This chapter also addresses the issues of soil liquefaction. Methods of analysis for soil liquefaction are presented, incorporating various techniques generally accepted by the profession. The consequences resulting from liquefaction, namely liquefaction-induced settlement, lateral spreading, and loss of bearing capacity, are presented as well as methods of estimating these effects. Various methods and strategies to mitigate the effects of soil liquefaction are presented as well as the merits of each. The latter part of the chapter discusses other geologic-seismic hazards, including seismic settlement, landsliding, tsunamis, and earthquake fault rupture. There is also a discussion of soil-structure interaction and design of walls below grade for seismic earth pressures.

3.1 INTRODUCTION

Structures come in different shapes, forms, and sizes. However, all structures have at least one feature in common; they all have a foundation. A foundation is the means by which the superstructure interfaces with the underlying soil or rock. Under static conditions, generally only the vertical loads of a structure need be transferred to the supporting soil or rock. In a seismic environment, the loads imposed on a foundation from a structure under seismic excitation can greatly exceed the static vertical loads or even produce uplift; in addition, there will be horizontal forces and possibly moments at the foundation level.

Consideration must also be given to what could happen to the supporting soil or rock under seismic excitation. For example, an earthquake might cause the phenomenon of liquefaction to occur in loose sandy soils which would cause a virtually complete loss of all bearing capacity of the soil; needless to say, a structure founded on such soils would suffer great distress and upset.

This chapter will attempt to identify those phenomena that would affect the design of foundations and structures in a seismic environment. Some of these phenomena can be effectively designed for by structural detailing, but some of these phenomena are beyond the magic and wizardry of the structural engineering profession and geotechnical wizardry may also be needed. In some instances, there may not be an economical engineering solution for the problem.

This chapter will be different from other chapters in this handbook in the respect that not all of the solutions to the seismic problems will be an engineering solution. This just points out the limitations of the science and art we know as engineering. We as engineers must be able to recognize our limitations and shortcomings and realize that we cannot always be the white knight that is able to save the damsel in distress. If we can attain at least this little enlightenment, we will all be better engineers.

In a seismic environment, there may exist a potential for ground failures. It is obvious that if the ground should fail beneath a structure, the structure could be severely or totally damaged. Such an event would threaten real property and life safety. Several different ground failure mechanisms will be discussed in this chapter.

3.2 SITE AND SOIL CONDITIONS

Because a foundation must be capable of adequately supporting a structure in an economical manner, it is imperative that there be a proper geotechnical investigation. This geotechnical investigation should provide information about the soil types beneath the site and their physical characteristics (i.e., strength, compressibility, permeability, etc.). The investigation should also provide economical and feasible alternatives for the support of the structure. These recommendations should take into account the functionality and purpose of the structure. In a seismic environment, the geotechnical investigation would also need to evaluate the behavior of the supporting soils under earthquake excitation and determine or predict the impact and consequences upon the structure and the foundation types recommended.

Not only is it important to investigate the soil conditions, the general site conditions also merit deep scrutiny. This investigation should include features near the building area and also distant features. Important nearby site features would include water levels, topographic features, and the presence of other structures both above and below ground. Offsite and even distant features could have some influence upon the proposed structure, especially in a seismically active area. For example, there could be large bodies of water retained by earth dams that could fail in an earthquake; if the structure is in the path of this potential inundation, the consequences could be very grave indeed.

3.3 SITE EFFECTS

3.3.1 Effects of Soils on Earthquake Loads on Structures

It has become recognized that the local site conditions have a very important role on the response of structures. The soil and rock at a site have specific characteristics that can significantly amplify the incoming earthquake motions traveling from the earthquake source. The importance of local site conditions was recognized in the 1960s by the influence of ground motions on midheight buildings in the Caracas, Venezuela earthquake. For buildings of about the same height with similar construction, it was observed that such buildings founded on deep soils were more damaged than the similar buildings founded on rock. These observations were further confirmed with the 1985 Mexico City earthquake where ground motions in Mexico City, some several hundreds of kilometers from the fault rupture, were amplified in the deep soft lakebed deposits that underlie the city; these ground motions had a long period and affected many high-rise buildings adversely with some collapses.

3.3.2 Uniform Building Code Recognition

The Uniform Building Code (UBC) acknowledged the importance of local site effects and the concept of a "Soil Factor" was added to the lateral force design procedure in the 1976 edition of the UBC.(3-1) At that time, a Soil-Structure Resonance Factor, S, was part of the design base shear equation; the value of the "S-factor" was dependent upon the ratio of T/T_s, where T is the fundamental building period and T_s is the characteristic site period. The "S-factor" ranged from a minimum of 1.0 to a maximum of 1.5. This concept of the soil factor remained in the UBC up to the 1985 edition(3-2) and was removed in the 1988 edition.(3-3)

In the 1985 edition, a second method of determining the Soil Factor was introduced. This method is not dependent on the ratio of T/T_s. Instead, the code defined three soil profile types, which essentially were rock, deep soil, and soft soil and the Soil Profile types were designated S_1, S_2, and S_3, respectively. The values of the Soil Factor were 1.0, 1.2, and 1.5 for S_1, S_2, and S_3, respectively. In response to the Mexico City earthquake, a fourth Soil Profile type, S_4, was added in 1988 for very deep soft soils like those found in Mexico City and perhaps in some parts of the San Francisco Bay region; the S_4 factor was equal to 2.0.

Uniform Building Code, 1994 Edition

The 1994 UBC(3-4) specifies the design base shear in a given direction to be:

$$V = \frac{ZICW}{R_w}$$

where $C = \dfrac{1.25\,S}{T^{2/3}}$

I = Importance Factor

Z = Seismic Zone Factor

The value of C need not exceed 2.75 and may be used for any structure without regard to soil type or structure period. The value of the Seismic Zone Factor, Z, is given in Table 3-1:

Table 3-1. — Seismic Zone Factor
From Table 16-I of the 1994 UBC (Ref. 3-4)

Zone	1	2A	2B	3	4
Z	0.075	0.15	0.20	0.30	0.40

The Site Coefficients, S, for the four soil types in the 1994 UBC are given in Table 3-2:

Table 3-2. — Site Coefficients, S
From Table 16-J of the 1994 UBC (Ref. 3-4)

TYPE	DESCRIPTION	S FACTOR
S_1	A soil profile with either: (a) A rock-like material characterized by a shear-wave velocity greater than 2,500 feet per second (762 m/s) or by other suitable means of classification, or (b) Medium-dense to dense or medium-stiff to stiff soil conditions, where soil depth is less than 200 feet (60,960 mm)	1.0
S_2	A soil profile with predominantly medium-dense to dense or medium stiff to stiff soil conditions, where the soil depth exceeds 200 feet (60,960 mm)	1.2
S_3	A soil profile containing more than 20 feet (6,096 mm) of soft to medium-stiff clay but not more than 40 feet (12,192 mm) of soft clay	1.5
S_4	A soil profile containing more than 40 feet (12,192 mm) of soft clay characterized by a shear wave velocity less than 500 feet per second (152.4 m/s)	2.0

The site factor is to be established from properly substantiated geotechnical data. In locations where the soil properties are not known in sufficient detail to determine the soil type, soil profile S_3 is to be used. Soil profile S_4 need not be assumed unless the building official determines that soil profile S_4 may be present at the site, or in the event that soil profile S_4 is established by geotechnical data.

Uniform Building Code, 1997 Edition

The 1997 UBC[3-5] has some major changes from the earlier editions. The first major difference is that it is a strength-based code. From an earth science or geotechnical perspective, the 1997 UBC has tried to incorporate new understanding about ground motion amplification and attempts to account for near-source effects.

The 1997 UBC contains a number of very significant changes affecting the seismic design of buildings. The code was developed by the Seismology Committee of the Structural Engineers Association of California (SEAOC) over a period of three years and is contained in Appendix C of the 1996 Recommended Lateral Force Requirements and Commentary, also known as the SEAOC Blue Book.[3-6] In addition to converting the code from a working stress to a strength basis, it was intended to advance the seismic provisions in several important areas. The Seismology Committee developed the proposal in coordination with a parallel effort by the Building Seismic Safety Council (BSSC) for the 1997 NEHRP Provisions.[3-7] (NEHRP is an acronym for the National Earthquake Hazards Reduction Program.) The NEHRP Provisions serve as the source document for other United States model building codes (BOCA and Southern Building Code). Therefore, this change is seen not only as an important advancement in seismic design requirements, but as a critical step toward the cooperative development of a single national building code for the United States by the year 2000.

The 1997 UBC code incorporates a number of important lessons from recent earthquakes and recent advances from other sources. In general it is intended to provide parity with previous requirements, except for longer period buildings in near-field locations and for structural systems with poor redundancy.

3.3.3 Overview of 1997 UBC

The following key concepts are contained in the 1997 UBC:

1. The adoption of ASCE-7 load factors for strength-based load combinations. In addition, working stress load combinations are maintained as an alternative.
2. The incorporation of a Redundancy/Reliability Factor (ρ), which is intended to encourage redundant lateral force resisting systems by penalizing non-

redundant ones through higher lateral force requirements.

3. The incorporation of near-source factors (N_a and N_v) in Seismic Zone 4 which are intended to recognize the amplified ground motions which occur at close distances to the fault.
4. The adoption of a new set of soil profile categories (from 1994 NEHRP) which are used in combination with Seismic Zone Factors (Z) and near-source factors, to provide site-dependent ground motion coefficients (C_a and C_v) defining ground motion response within the acceleration and velocity-controlled ranges of the spectrum. The design response spectrum differs from the spectrum in the 1994 and earlier UBC in two ways: the constant velocity portion is now defined by 1/T, as opposed to $1/T^{2/3}$, causing it to drop more rapidly in that range, and the plateau in the constant acceleration domain varies with C_a rather than being a constant value for all soil profiles.
5. Substantial revisions to lateral force requirements for elements of structures, nonstructural components and equipment supported by structures. These provisions more accurately represent lateral forces on elements by recognizing varying diaphragm accelerations, component amplification, component response modification, and ground motion response. Similar changes are proposed for non-building structures.
6. A simplified design base shear calculation permitted for one- and two-story dwellings, one to three-story light frame construction and other one- and two-story buildings as permitted.
7. The R-factor has been adjusted to provide a strength level base shear. Earlier editions of the code change proposal submitted to the International Conference of Building Officials (ICBO) contained a two-component R-factor, with values for R_0 and R_d representing overstrength and system ductility. However, it was found that the requirements for defining the plastic mechanism analysis required for the R_0 calculation could not be codified in simple language while guaranteeing accuracy, so the single R value was adopted. However, the two component R has been maintained in the SEAOC Blue Book version, essentially for its educational value.

The N_a and N_v factors represent the most significant difference between the 1997 UBC and the developing 1997 NEHRP Provisions, which will address near field effects through the use of spectral values maps which are being developed by BSSC based on new seismic risk maps developed by the United States Geological Survey (USGS). The maps represent a major research effort which was not completed (for design application) in time for use in the 1997 UBC code.

An important concept in the 1997 UBC code is the use of *elastic response parameters* to define unreduced forces and displacements (R=1) for calculations involving drift and deformation compatibility and in dynamic analysis. In addition, the parameter E_M has been introduced to represent the maximum earthquake force that can be developed in the structure for use in addressing non-ductile conditions, similar to the $3R_W/8$ parameter in the 1994 UBC. E_M is used to define collector strength requirements.

Near-Source Factors and Code Elastic Design Response Spectra

The design base shear, as determined in the 1994 and earlier editions of the UBC, is a function of an assumed level of ground motion. In Seismic Zone 4, this level of ground motion has been taken as being an effective peak ground acceleration (EPA) of 0.4g. While no formal relationship exists between the EPA and the peak ground acceleration (PGA), it may be taken that the EPA is about two-thirds of the PGA.

Strong motion measurements in recent large earthquakes, such as the 1994 Northridge and 1995 Kobe events, showed that ground motions are significantly greater near the earthquake source. These events had near-source ground

Table 3-3. — Soil Profile Types, 1997 UBC
From Table 16-J, 1997 UBC (Ref. 3-5)

Soil Profile Type	Soil Profile Name/Generic Description	Average Shear Wave Velocity, v_s, for upper 100 feet of soil profile, feet/second (m/s)
S_A	Hard Rock	>5,000 (1,500)
S_B	Rock	2,500 to 5,000 (760 to 1,500)
S_C	Very Dense Soil and Soft Rock	1,200 to 2,500 (360 to 760)
S_D	Stiff Soil	600 to 1,200 (180 to 360)
S_E	Soft Soil	<600 (180)
S_F	Soils Requiring Site-Specific Evaluation	

motions that greatly exceeded the EPA level for Zone 4 in the 1994 UBC codes. It has also been observed that the amplification of long-period ground motions is also greater with less competent site soil conditions.

These near-source factors apply only to Seismic Zone 4 because it is believed that the near-source effect is only significant for large earthquakes. Research of the ground motions from Northridge, Kobe, and other events have indicated that the amount of near-source effect is greater at the long periods than the short periods. Therefore, two near-source factors were introduced that result in a greater amplification of the ground motions for long periods than for those for short periods. The near-source factors were introduced in the 1997 UBC strength-based seismic code to account for this increase as a function of the earthquake potential of a known earthquake source and the distance from source to the given site.

As mentioned earlier, a new set of soil profile types has been introduced into the 1997 UBC. These soil profile types are based on the average soil properties for the upper 100 feet of the soil profile. An abbreviated description as a function of the average shear wave velocity in the upper 100 feet (approximately 30 meters) is given in Table 3-3 for five "stable" profile types, designated as S_A through S_E; there is a sixth profile type (S_F) which require a site-specific evaluation. The near-source factor, N_a, for short periods is shown in Table 3-4 as a function of the three seismic source types; the near-source factor, N_v, for long periods is shown in Table 3-5 for the different seismic source types.

The types of soils requiring site-specific evaluation in Soil Profile Type S_F are:

1. Soil vulnerable to potential failure or collapse under seismic loading such as liquefiable soils, quick and highly sensitive clays, collapsible weakly cemented soils.
2. Peats and/or highly organic clays [H > 10 feet of peat and/or highly organic clay, where H = thickness of soil].
3. Very high plasticity clays [H > 25 feet with Plasticity Index > 75].
4. Very thick soft/medium stiff clays [H > 120 feet].

The closest distance to the seismic source is to be taken as the minimum distance between the site and the area described by the vertical projection of the source on the ground surface (i.e., surface projection of the fault plane). For dipping faults, the surface projection is to include those portions of the source within 10 km of the surface as illustrated in Figure 3-1. The definitions of the seismic source types are shown in Table 3-6. For seismic sources

Table 3-5. Near-Source Factor for Short Periods, N_a
From Table 16-S, 1997 UBC (Ref. 3-5)

Seismic Source Type	Closest Distance to Known Seismic Source		
	≤ 2 km	5 km	≥ 10 km
A	1.5	1.2	1.0
B	1.3	1.0	1.0
C	1.0	1.0	1.0

Table 3-6. — Near-Source Factor for Long Periods, N_v
From Table 16-T, 1997 UBC (Ref. 3-5)

Seismic Source Type	Closest Distance to Known Seismic Source			
	≤ 2 km	5 km	≥ 10 km	≥ 15 km
A	2.0	1.6	1.2	1.0
B	1.6	1.2	1.0	1.0
C	1.0	1.0	1.0	1.0

Table 3-4. — Seismic Source Type
From Table 16-U, 1997 UBC (Ref. 3-5)

Seismic Source Type	Seismic Source Description	Seismic Source Definition	
		Maximum Moment Magnitude, *M*	Slip Rate, *SR* (mm/yr)
A	Faults that are capable of producing large magnitude events and which have a high rate of seismic activity.	$M \geq 7.0$ and	$SR \geq 5$
B	All faults other than Types A or C.	$M \geq 7.0$ and $M < 7.0$ and $M \geq 6.5$ and	$SR < 5$ $SR > 2$ $SR < 2$
C	Faults which are not capable of producing large magnitude earthquakes and which have a relatively low rate of seismic activity.	$M < 6.5$ and	$SR \leq 2$

capable of larger earthquakes and having a higher seismicity or slip rate, the near-source factors are higher than for faults capable of lesser maximum earthquakes or with lower slip rates. Faults or seismic sources with lower maximum moment magnitude and low slip have N-factors with the value of unity (1.0).

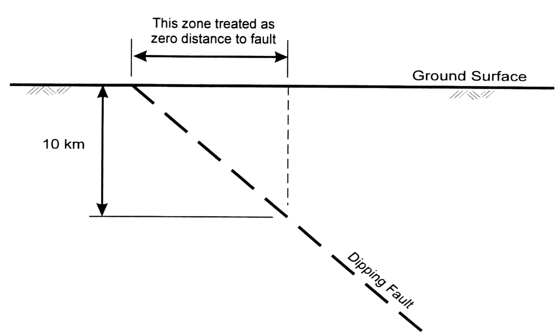

Figure 3-1. Treatment of Dipping Faults

Table 3-7. — Seismic Coefficient, C_a
From Table 16-Q, 1997 UBC (Ref. 3-5)

Soil Profile Type	Seismic Zone Factor, Z				
	Z = 0.075	Z = 0.15	Z = 0.2	Z = 0.3	Z = 0.4
S_A	0.06	0.12	0.16	0.24	$0.32N_a$
S_B	0.08	0.15	0.20	0.30	$0.40N_a$
S_C	0.09	0.18	0.24	0.33	$0.40N_a$
S_D	0.12	0.22	0.28	0.36	$0.44N_a$
S_E	0.19	0.30	0.34	0.36	$0.36N_a$

Table 3-8. — Seismic Coefficient, C_v
From Table 16-R, 1997 UBC (Ref. 3-5)

Soil Profile Type	Seismic Zone Factor, Z				
	Z = 0.075	Z = 0.15	Z = 0.2	Z = 0.3	Z = 0.4
S_A	0.06	0.12	0.16	0.24	$0.32N_v$
S_B	0.08	0.15	0.20	0.30	$0.40N_v$
S_C	0.13	0.25	0.32	0.45	$0.56N_v$
S_D	0.18	0.32	0.40	0.54	$0.64N_v$
S_E	0.26	0.50	0.64	0.84	$0.96N_v$

The Seismic Coefficients, C_a and C_v, are shown in Tables 3-7 and 3-8. As mentioned earlier, the near-source factor is only applicable in Seismic Zone 4, and only the seismic coefficients for Zone 4 are dependent on the near-source factors. The International Conference of Building Officials has published a set of maps defining the near-source zones in the state of California and adjacent portions of Nevada.(3-8)

The total design base shear, V, in a given direction is determined by the following equation:

$$V = \frac{C_V I}{RT} W$$

where I = importance factor
W = total seismic dead load
R = numerical coefficient representative of ductility and overstrength
T = fundamental period of vibration, in seconds

This formula defines the long period or constant velocity range.

For short periods (i.e., $T < C_v / 2.5C_a$), the following equation defines the constant acceleration range:

$$V = \frac{2.5 C_a I}{R} W$$

In addition, for Seismic Zone 4, the total base shear is also governed by a minimum "floor" value at longer periods by the following equation:

$$V = \frac{0.8 Z N_V I}{R} W$$

The elastic design response spectra, as defined by C_a and C_v, is shown in Figure 3-2. Figure 3-3 shows a comparison of the basic elastic design response spectra for UBC Seismic Zones 1, 2A, 2B, 3 and 4 for Soil Profile Type S_D; this profile type is probably the most common soil profile in most of California. For this comparison, the near-source factors have both been assumed to have a value of unity (1.0). The floor caused by the special Zone 4 restriction is misleading

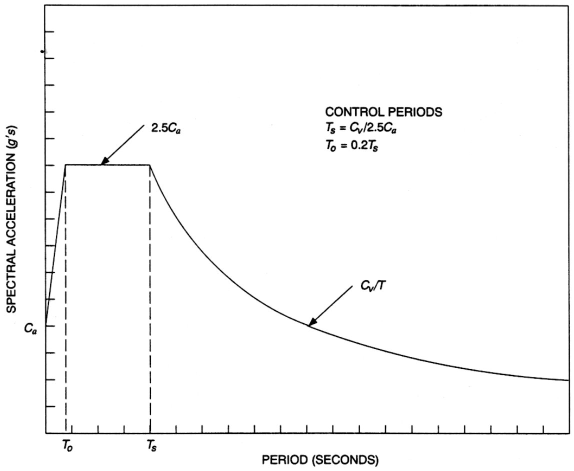

Figure 3-2. 1997 UBC Design Response Spectra. From Figure 16-3, 1997 UBC (Ref. 3-5)

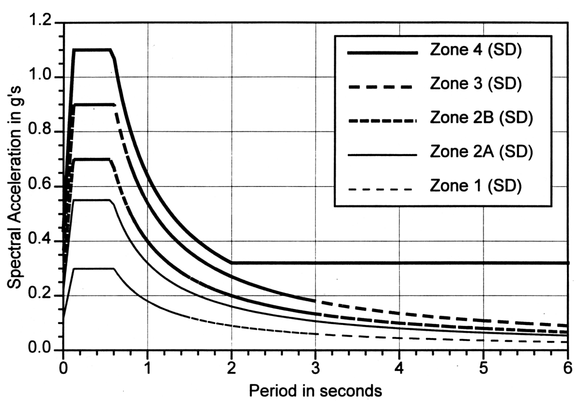

Figure 3-3. Response Spectra, UBC 1997 Edition, Soil Profile Type S_D

as the base shear computed from the design response spectrum will be greatly reduced when the "R" factor is divided through. There is another long period minimum "floor" value (that is not reduced by "R") that applies to all seismic zones that the total base shear should not be less than the following:

$$V = 0.11\, C_a I\, W$$

With this additional minimum "floor," the differences in the base shear for longer periods between Zone 4 and the lesser zones at the longer structural periods are somewhat reduced.

Figure 3-4 shows a comparison of the elastic response spectra for the five stable soil profile types (S_A through S_E) for only Zone 4 assuming both near-source factors to be equal to unity (1.0). It is unlikely that Soil Profile Type S_A would exist in any significant metropolitan area in California. It should be noted that the spectral accelerations are larger at longer periods as the soil profile types become softer. The "floor" minimum spectral acceleration is the same regardless of soil profile type.

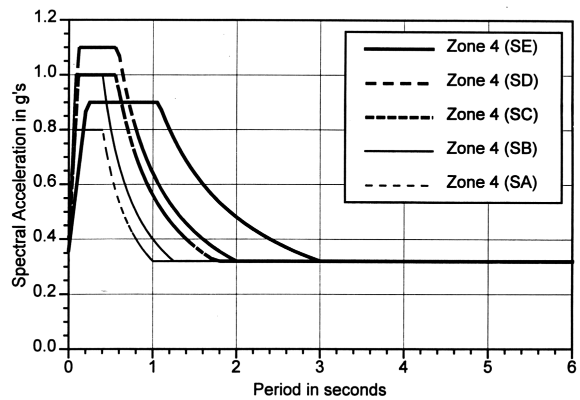

Figure 3-4. Response Spectra, Uniform Building Code 1997 Edition, Zone 4, $N_a = N_v = 1.0$ [After Lew and Bonneville (Ref. 3-9)]

Figure 3-5 compares the elastic response spectra in Zone 4 for a Soil Profile Type S_D for distances from a site to a Seismic Source A, the most active faults. The elastic response spectra for distances of less than 2, 5, 10, and 15 km are shown; at a distance of 15 km or greater, both N_a and N_v are equal to unity (1.0). Sites near a Seismic Source A will be subject to design base shears significantly greater than presently prescribed in the 1994 UBC. Similar plots of the elastic design response spectra for soil profile S_D near a Seismic Source Type B for distances of less than 2, 5, and 10 km are shown in Figure 3-6.

The California State Geologist has prepared near-source maps for the State of California for implementation with the adoption of the 1997 UBC. Near-source effects are only considered

Table 3-9. — Additional Definitions for Soil Profiles S_C through S_E (Ref. 3-5)

Soil Profile Type	Average Standard Penetration Blow Count	Average Undrained Shear Strength (pounds per square ft)	Average Undrained Shear Strength (kPA)
S_C	>50	>2,000	>100
S_D	15 to 50	1,000 to 2,000	50 to 100
S_E	<15	>10 feet of soft clay with PI > 20, w_{mc} > 40%, and s_u < 500 psf	>3048 mm of soft clay with PI > 20, w_{mc} > 40%, and s_u < 500 psf

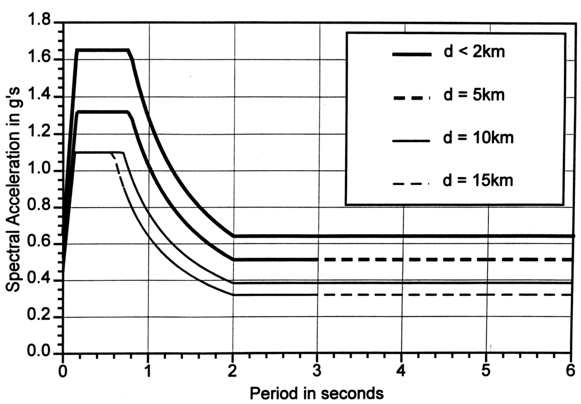

Figure 3-5. Response Spectra, Uniform Building Code 1997 Edition Zone 4, Seismic Source A, and Soil Profile Type S_D [After Lew and Bonneville (Ref. 3-9)]

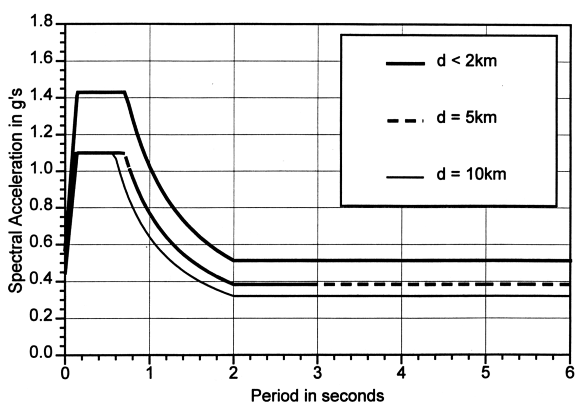

Figure 3-6. Response Spectra, Uniform Building Code 1997 Edition Zone 4, Seismic Source B, and Soil Profile Type S_D [After Lew and Bonneville (Ref. 3-9)]

in Zone 4, thus, only parts of California, Hawaii and Alaska are affected in the United States.

Site Categorization Procedure

As mentioned in the previous section, there are six soil profile types of the 1997 UBC as given in Table 3-3. Only an abbreviated definition in terms of shear wave velocity for the soil profile types was given. The additional 1997 UBC definitions for soil profiles S_C through S_E are given below in Table 3-9.

When the soil properties are not known in sufficient detail to determine the soil profile type, the Code specifies that Type S_D be used. Soil Profile Type S_E need not be assumed unless the local building official determines that Soil Profile Type S_E may be present at the site or in the event that Type S_E is established by geotechnical data.

Determination of the Average Shear Wave Velocity

This assumes that the shear wave velocity profile will be known for the upper 100 feet (30.48 m). The average shear wave velocity, v_s, is determined by the following formula:

$$\bar{v}_s = \frac{\sum_{i=1}^{n} d_i}{\sum_{i=1}^{n} \frac{d_i}{v_{si}}}$$

where:

d_i = thickness of Layer i in feet (or meters)

v_{si} = shear wave velocity in Layer i in feet/second (meters/second)

Determination of the Average Standard Penetration Resistance

The 1997 UBC defines the average field standard penetration resistance, N, and the average standard penetration resistance for cohesionless soil layers, N_{CH}, by the following formulae:

$$\bar{N} = \frac{\sum_{i=1}^{n} d_i}{\sum_{i=1}^{n} \frac{d_i}{N_i}}$$

$$\bar{N}_{CH} = \frac{d_i}{\sum_{i=1}^{n} \frac{d_i}{N_i}}$$

where:

d_i = thickness of Layer i in feet (or millimeters)

d_s = the total thickness of cohesionless soil layers in the top 100 feet (30,480 millimeters)

N_i = the standard penetration resistance of soil layer in accordance with approved nationally recognized standards

Determination of Average Undrained Shear Strength.

The average undrained shear strength, S_u, is to be determined by the following equation:

$$\bar{S}_u = \frac{d_c}{\sum_{i=1}^{n} \frac{d_i}{S_{ui}}}$$

where:

d_c = the total thickness (100 – d_s) of cohesive soil layers in the top 100 feet (30,480 millimeters)

S_{ui} = the undrained shear strength in accordance with approved nationally recognized standards, not to exceed 5,000 psf (250 kPa)

3.3.4 Site Profile Examples–1994 UBC

Example 1

The soil profile at a site of a proposed hospital has been described as being interlayered beds of medium dense to dense sands and medium stiff to stiff clays. The thickness of the interlayered beds is 250 feet, at which depth, bedrock with a shear wave velocity of 2,500 feet/second is encountered. Determine the appropriate S Factor in accordance with the 1994 UBC.

Solution: Per Table 3-2 (Table 16-J, 1994 UBC), the profile type is S_2, corresponding to an S Factor of 1.2.

Example 2

The soil profile is similar to that described in Example 1, except that the bedrock is shallower, at a depth of 127 feet. Determine the appropriate S Factor in accordance with the 1994 UBC.

Solution: Per Table 3-2, Profile Type S_1, S=1.0.

Example 3

A site on reclaimed land near a river is being developed for a major commercial center. The geotechnical investigation, including a downhole seismic survey, revealed the typical shear wave velocity profile in the upper 200 feet to be:

Depth (feet)	Soil Description	Shear Wave Velocity (ft/sec)
0–15	Fill, silty sand	600
15–25	Highly plastic soft clay	300
25–50	Plastic, soft clay	450
50–75	Medium stiff clay	750
75–100	Medium stiff clay	1,000
100–150	Stiff clay	1,400
150–200	Dense sand and gravel	1,650

Determine the appropriate S Factor in accordance with the 1994 UBC.

<u>Solution:</u> From 15 to 50 feet, there are 35 feet of soft clays having a shear wave velocity of less than 500 feet per second; based on the description, profile is type S_3, with S=1.5.

Example 4

A site on San Francisco Bay is being considered for a major high-rise building. The geotechnical investigation has established the typical soil profile at the site to be:

Depth (feet)	Soil Description	Shear Wave Velocity (ft/sec)
0–10	Compacted fill, sandy clay	650
10–60	Young bay mud, soft	350
60–100	Older bay mud, medium stiff	1,000
100–150	Older bay mud, stiff	1,400
>150	Franciscan Formation bedrock	2,000

Determine the appropriate S Factor in accordance with the 1994 UBC.

<u>Solution:</u> Profile contains more than 40 feet of soft clay with shear wave velocity of less than 500 ft/sec; therefore, site profile is type S_4, and S=2.0.

3.3.5 Site Profile Examples–1997 UBC

Example 1

The soil profile at a site of an industrial facility has been investigated and the typical soil profile in the 100 feet has been determined to be:

Depth (feet)	Soil Description	Shear Wave Velocity	"N"	PI
0–30	Clay	-	-	80
30–50	Silty Sand	-	35	-
50–100	Sand and Gravel	-	50	-

Determine the appropriate soil profile type.

<u>Solution:</u> Based on the clay layer with a PI > 75 and H > 25 ft, this profile type is S_F, requiring site-specific evaluation.

Example 2

A site is underlain by bedrock having a measured shear wave velocity of 1,800 m/s in the upper 30 m (100 ft). Determine the appropriate soil profile type.

<u>Solution:</u> Soil profile type is S_A, since $v_S >$ 1,500 m/sec.

Example 3

A soil profile has the following description from the boring logs:

Depth (feet)	Soil Type	N-value
0–20	Sand	10
20–40	Sand	12
40–60	Sand	15
60–100	Sand	18

Determine the appropriate soil profile type.

<u>Solution:</u> Determine $\overline{N}$, the average field standard penetration resistance

$$\bar{N} = \frac{\sum_{i=1}^{n} d_i}{\sum_{i=1}^{n} \frac{d_i}{N_i}} = \frac{20'+20'+20'+40'}{\frac{20'}{10}+\frac{20'}{12}+\frac{20'}{15}+\frac{40'}{18}}$$

$$\bar{N} = \frac{100}{2.0+1.67+1.33+2.22} = \frac{100}{7.22} = 13.9$$

Since $\overline{N}$ is < 15, soil profile type is S_E.

Example 4

Given a soil profile:

Depth (feet)	Soil Type	N-value
0–10	Sand	25
10–30	Sand	40
30–75	Sand	60
75–100	Sand	70

Determine the appropriate soil profile type.

Solution:

$$\bar{N} = \frac{\sum_{i=1}^{n} d_i}{\sum_{i=1}^{n} \frac{d_i}{N_i}} = \frac{10'+20'+45'+25'}{\frac{10'}{25}+\frac{20'}{40}+\frac{45'}{60}+\frac{25'}{70}}$$

$$\bar{N} = \frac{100}{0.40+0.50+0.75+0.36} = \frac{100}{2.01} = 49.8$$

Since $15 \le N \le 50$, soil profile type is S_D.

Example 5

The soil profile at a site has been determined to be:

Depth (feet)	Soil Type	N-value	Average Undrained Shear Strength (kPa)
0–10	Fill, dense sand	50	–
10–20	Clay	–	75
20–50	Clay	–	100
50–60	Clay	–	120
60–100	Clay	–	160

Determine the appropriate soil type.

Solution:

Ignore the upper 10 feet of the profile, consider just the clays.

$$\bar{S}_u = \frac{d_c}{\sum_{i=1}^{n} \frac{d_i}{s_{ui}}} = \frac{100-d_s}{\sum_{i=1}^{n} \frac{d_i}{s_{ui}}}$$

$$= \frac{100'-10'}{\frac{10'}{75\,kPa}+\frac{30'}{100\,kPa}+\frac{10'}{120\,kPa}+\frac{40'}{160\,kPa}}$$

$$= \frac{90}{0.13+0.30+0.08+0.25} = \frac{90}{0.77}$$

$$= 117.4\,kPa$$

Therefore, soil profile type is S_C.

3.3.6 Near-Source Factor Examples–1997 UBC

Example 1

For a building site located in the City of Palmdale, 1.1 km from the San Andreas fault, determine the Near-Source Factors, N_a and N_v. Note: the San Andreas fault has a maximum moment magnitude of about 8¼ and an annual slip rate of 25 mm/yr.

Solution:

Seismic Source Type: The San Andreas fault is classified as a Type A seismic source (Table 3-6)

Per Table 3-4, Near-Source Factor, N_a, = 1.5
Per Table 3-5, Near-Source Factor, N_v, = 2.0

Example 2

For the site classified in Example 1, determine the seismic coefficients, C_a and C_v, if the soil profile is type S_D. Note: Palmdale is in Seismic Zone 4 where the Seismic Zone Factor, Z = 0.4.

Solution:

Per Table 7, $C_a = 0.44\ N_a = 0.44\ (1.5) = 0.66$
Per Table 8, $C_v = 0.67\ N_v = 0.67\ (2.0) = 1.34$

Example 3

A site is located in West Los Angeles, 7.5 km from the Newport-Inglewood fault (M=7.0, SR=1 mm/yr). The site profile is S_C and the site is in Seismic Zone 4. Determine the seismic coefficients, C_a and C_v.

Solution:

– The Newport-Inglewood fault is a seismic source Type B.
– Near-Source Factor, N_a = 1.0 for 7.5 km distance.
– Near-Source Factor, N_v = 1.1 for 7.5 km distance by interpolation.

For Z = 0.4 and S_C site,
$C_a = 0.40\ N_a = 0.40\ (1.0) = 0.40$
$C_v = 0.56\ N_v = 0.56\ (1.1) = 0.616$

Example 4

A site is located in the California desert; the closest active faults are 3.0 and 5.0 km from the site. Information on the faults are given as:

Fault	Distance (km)	Max. Magnitude	Slip Rate (mm/yr)
1	3.0	6.5	1.0
2	5.0	7.0	5.0

Determine the appropriate Near-Source Factors, N_a and N_v.

Solution:

By Table 3-6:
Fault 1 is a seismic source Type B
Fault 2 is a seismic source Type A

From Tables 3-4 and 3-5, the Near-Source Factors are:

Fault	N_a	N_v
1	1.2	1.47
2	1.2	1.6

Use the maximum values; therefore, N_a = 1.2; N_v = 1.6.

Example 5

The recently discovered Bachman blind thrust fault was found to underlie the site of a new building development. Seismologists have estimated the fault properties and geometry to be:

1. Buried thrust fault with a 45° dip.
2. Maximum magnitude = 7.5.
3. Maximum annual slip rate = 10 mm/yr.
4. Fault orientation relative to site is shown in the figure below.

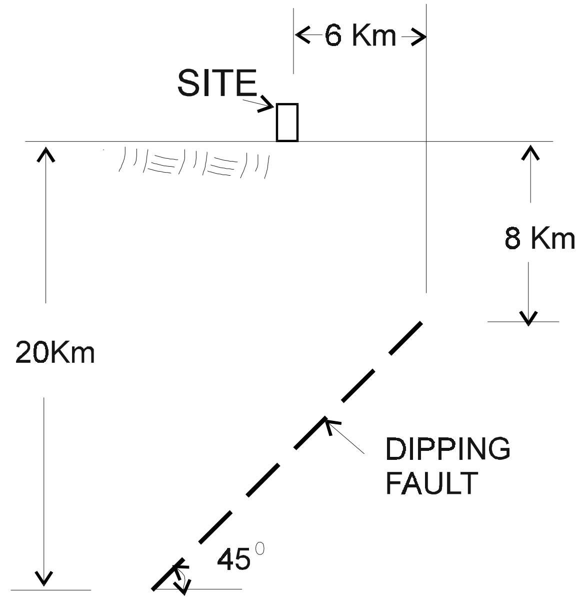

Determine the Near-Source Factors, N_a and N_v.

Solution:

The Bachman fault, per Table 3-6, is a seismic source Type A. The surface projection of fault above a 10 km depth is shown below:

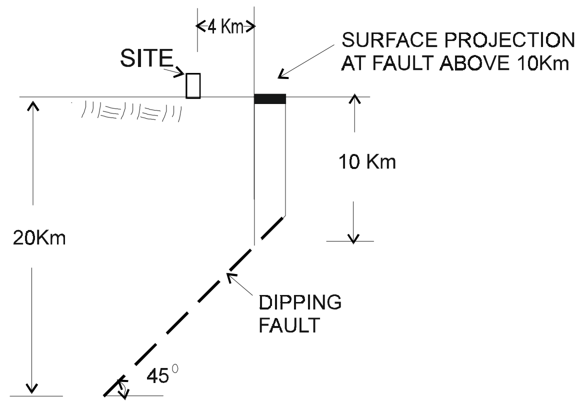

For Type A source and 4 km distance,
N_a = 1.3 (Table 3-4) and N_v = 1.73 (Table 3-5)

3.3.7 NEHRP 1997 Recommended Provisions for Seismic Regulations

The NEHRP Recommended Provisions for Seismic Regulations for New Buildings and Other Structures(3-7) present criteria for the design and construction of structures to resist earthquake ground motions. The NEHRP 1997 Provisions form the basis of the seismic provisions for the proposed unified national building code for the United States to be called the International Building Code (IBC)(3-10).

3.3.8 2000 International Building Code Seismic Requirements

The International Building Code (IBC), 2000 edition (3-10) has recently been published. It represents a cooperative effort to bring national uniformity to the building codes in the United States. The IBC code has been developed jointly by the International Code Council, which consists of the Building Officials and Code Administrators International, Inc. (BOCA), the International Conference of Building Officials (ICBO), and the Southern Building Code Congress International (SBCCI).

There are new earthquake definitions, assumptions, and procedures in the 2000 IBC, based on the 1997 NEHRP. The IBC specifies a procedure to establish ground motion accelerations, represented by response spectra and coefficients derived from those spectra. The design earthquake (DE) ground motions have been defined as being two-thirds of the Maximum Considered Earthquake (MCE) ground motions:

$$DE = \frac{2}{3} MCE$$

The MCE is defined as the "most severe earthquake effects" considered by the IBC, and is essentially the "worst case" earthquake, which has been used for design of special (base isolated) buildings or for collapse check of existing buildings (such as defined in FEMA 273). The DE is the "design-basis" earthquake for conventional building design, with margins provided by the inherent conservatisms built into the NEHRP Provisions.

2000 IBC Seismic Base Shear Equation

The seismic base shear, V, in a given direction is to be determined by the following equation:

$$V = C_s W$$

Where:

C_s = seismic response coefficient
W = total dead load plus applicable portions of other loads as defined in IBC

The seismic response coefficient, C_s, is determined by the equation:

$$C_s = \frac{S_{DS}}{(R/I_E)}$$

where:

S_{DS} = the design spectral response acceleration at short periods
R = response modification factor defined in the IBC
I_E = occupancy importance factor defined in IBC and ranges from 1.0 to 1.5

The response modification factor, R, depends on the type of building system and ranges from a value of 1½ for ordinary plain masonry wall systems to values of 7 to 8 for steel eccentrically braced frame systems. The value of the seismic response coefficient C_s as shown above need not exceed the following:

$$C_s = \frac{S_{D1}}{(R/I_E)T}$$

but shall not be taken less than:

$$C_s = 0.044\, S_{DS} I_E$$

For buildings and structures in Seismic Design Categories E or F, and those buildings and structures for which the 1 second spectral response, S_1, is equal to or greater than 0.6g, the value of C_s shall not be taken as less than:

$$C_s = \frac{0.5S_1}{R/I_E}$$

where:

S_{D1} = the design spectral response acceleration at 1 second period
T = fundamental period of the building (seconds)
S_1 = maximum considered earthquake spectral response acceleration at 1 second period

Seismic Design Categories E and F are assigned to structures in mapped areas with spectral response acceleration at a period of 1 second, S_1, exceeding 0.75g. It appears that where S_1 will be less than 0.75g in Seismic Zone 4, it will not be less than 0.60g; in this case, the structures will be assigned to Seismic Design Category D. [The seismic design categories are not discussed here, but suffice it to say that structures in Seismic Zone 4 will be either Seismic Design Category D, E, or F, which have more stringent requirements than Categories A, B, or C.]

2000 IBC Determination of Seismic Coefficient

The seismic coefficient, C_s, for the seismic base shear equation, is derived from a response spectra. This response spectra can be derived from a site-specific study or can be determined with the procedure in the 2000 IBC. In the 2000 IBC, the 5% damped response spectra is constructed from the "mapped maximum considered earthquake spectral response acceleration" at two points. One point, denoted as S_S, corresponds to short periods and the other point, denoted as S_1, corresponds to a 1 second period. The "mapped maximum considered earthquake spectral response acceleration" corresponds to a "soft rock" (Site Class B) condition; factors are applied to account for the site conditions to develop an appropriate response spectra. Another factor is applied to arrive at the final design response spectra.

2000 IBC Mapped Maximum Considered Earthquake Spectral Response Accelerations

The maximum considered earthquake spectral response acceleration for short period (0.2 seconds) and 1.0 second period are found on maps that are found in the 1997 NEHRP Provisions. Smaller scale versions of these maps are reproduced in the 2000 IBC. These maps were developed by the Building Seismic Safety Council (BSSC) and the United States Geological Survey (USGS) for the Federal Emergency Management Agency (FEMA). The maps are based on probabilistic seismic hazard analyses using fault source models developed by the USGS. The analyses were made for the 5% damped spectral response at 0.2- and 1.0-second periods corresponding to the ground motions having a 2 percent probability of being exceeded in 50 years; this is about a 2,500 year return period. This risk level is now referred to as the "maximum considered earthquake." Because of the tendency of probabilistic analyses to predict ground motions that greatly exceed what has been experienced, due mostly to the uncertainties in the seismic parameters and the long return period, a cap or limiting value was imposed on the spectral ordinates in the more seismically active areas of the United States, such as California. The probabilistic spectral response values were capped by the "deterministic maximum considered earthquake ground motion."

The soil class assumed in the analyses is a soil class B; the *Soil Classes* used in the IBC are the same as the *Soil Profile Types* used in the 1997 UBC. (The 1997 UBC adopted the NEHRP soil profile types.)

The deterministic maximum considered earthquake ground motion spectral response is to be calculated by taking into account the characteristic earthquake on any known fault within the region that has a slip rate exceeding 1 mm per year. The spectral response for 5% damping is to be calculated using a mean-plus-one standard deviation ground motion

Table 3-10. — Values of Site Coefficient F_a as a Function of Site Class and Mapped Spectral Response Acceleration at Short Periods, S_S (Ref. 3-10)

	Mapped Spectral Response Acceleration at Short Periods				
Site Class	$S_S \leq 0.25$	$S_S = 0.50$	$S_S = 0.75$	$S_S = 1.0$	$S_S \geq 1.25$
A	0.8	0.8	0.8	0.8	0.8
B	1.0	1.0	1.0	1.0	1.0
C	1.2	1.2	1.1	1.0	1.0
D	1.6	1.4	1.2	1.1	1.0
E	2.5	1.7	1.2	0.9	a
F	a	a	a	a	a

Note: Use straight-line interpolation for intermediate values of mapped spectral acceleration at short periods, S_S.

[a] Site-specific geotechnical and dynamic site response analysis should be performed to determine appropriate values.

Table 3-11. — Values of Site Coefficient F_v as a Function of Site Class and Mapped Spectral Response Acceleration at 1 Second Period, S_1 (Ref. 3-10)

	Mapped Spectral Response Acceleration at 1 Second Period				
Site Class	$S_S \leq 0.1$	$S_S = 0.2$	$S_S = 0.3$	$S_S = 0.4$	$S_S \geq 0.5$
A	0.8	0.8	0.8	0.8	0.8
B	1.0	1.0	1.0	1.0	1.0
C	1.7	1.6	1.5	1.4	1.3
D	2.4	2.0	1.8	1.6	1.5
E	3.5	3.2	2.8	2.4	a
F	a	a	a	a	a

Note: Use straight-line interpolation for intermediate values of mapped spectral acceleration at 1.0 second period, S_1.

[a] Site-specific geotechnical and dynamic site response analysis should be performed to determine appropriate values.

attenuation relationship. These deterministically spectral response values are used as upper bound values in the IBC maps.

Maps for Southern California have been developed and are shown in Figures 3-7 and 3-8. From the first map, the mapped maximum considered earthquake spectral response acceleration for short period, S_S, is found based on the location of the site. The second map is used to determine the mapped maximum considered earthquake spectral response acceleration for a 1-second period, S_1.

2000 IBC Adjustments to Spectral Response for Site Class Effects

As the S_s and S_1 values correspond to a Site Class B, adjustments must be made if the site in question is other than an Site Class B profile. The S_S and S_1 values are adjusted for site effects by the following formulas:

$$S_{MS} = F_a S_S$$

$$S_{M1} = F_v S_1$$

where:

F_a = site coefficient for short period response
F_v = site coefficient for 1 second period response

The values of the site coefficients F_a and F_v are given in Tables 3-10 and 3-11.

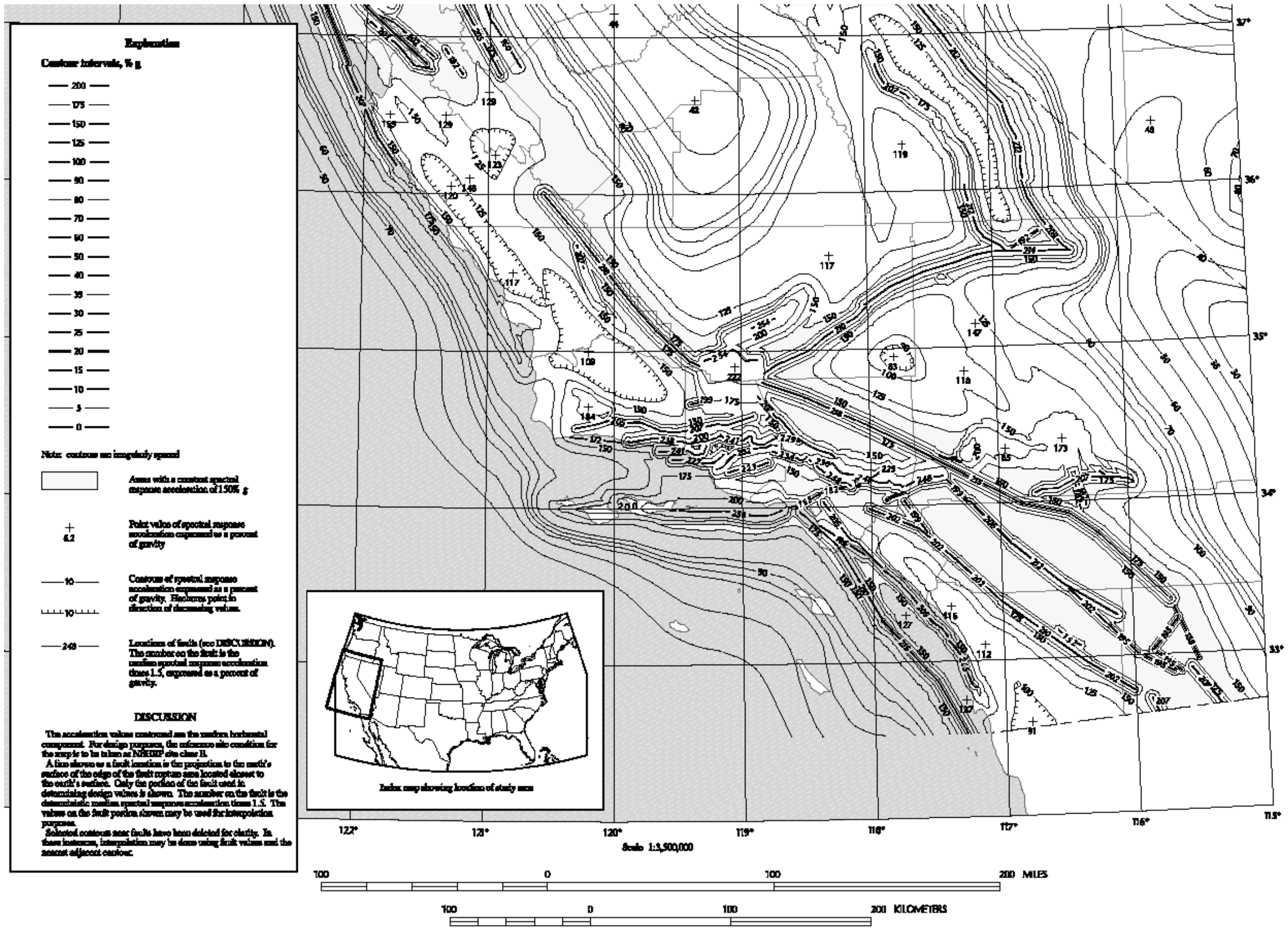

Figure 3-7. Maximum Considered Earthquake Ground Motion for Southern California:
Short (0.2 second) Period Spectral Response Acceleration (%g); Site Class B [After International Code Council, 2000 (Ref 3-10)]

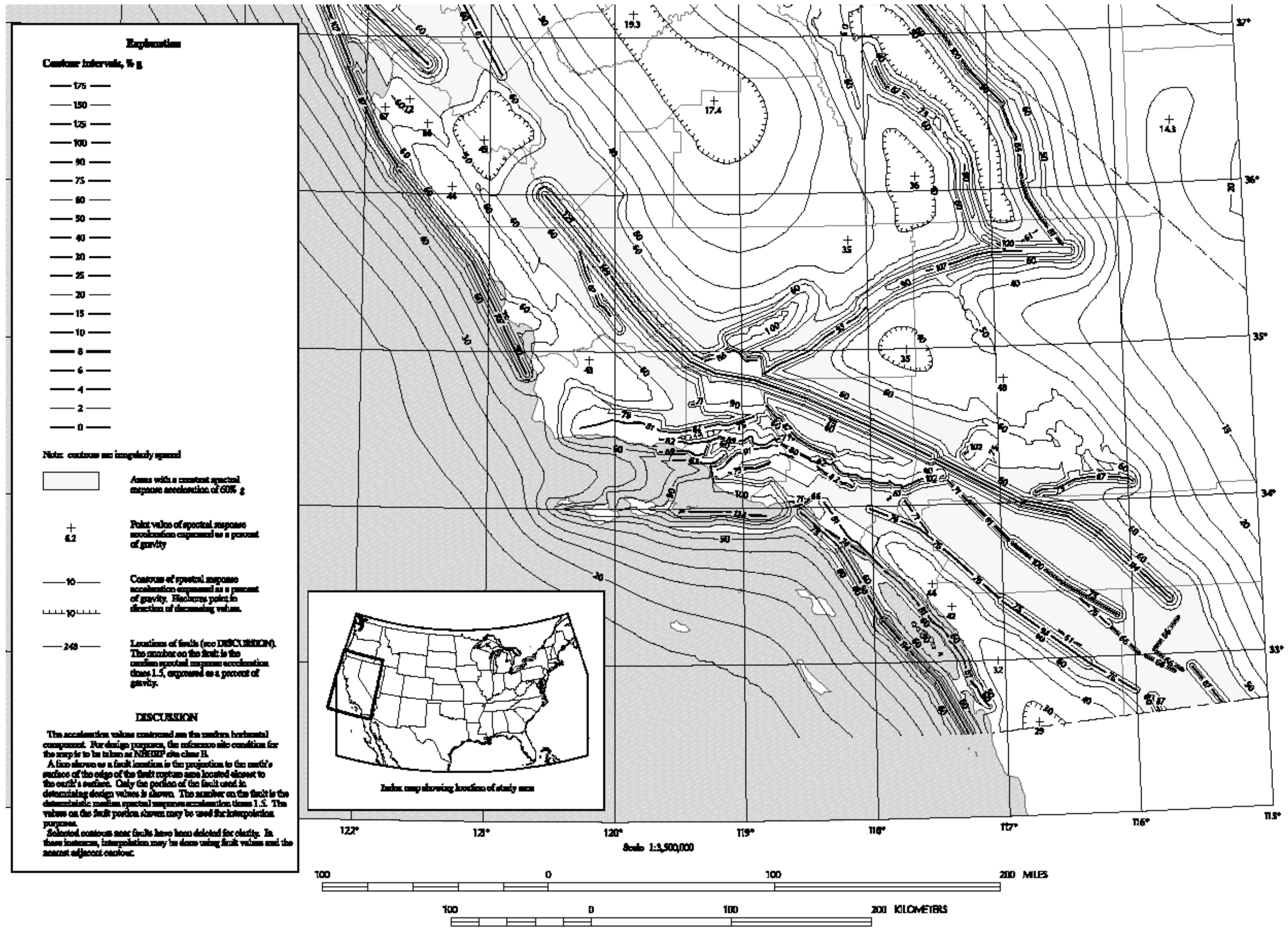

Figure 3-8. Maximum Considered Earthquake Ground Motion for Southern California:
1 Second Period Spectral Response Acceleration (%g); Site Class B [After International Code Council, 2000 (ref. 3-10)]

2000 IBC General Design Response Spectrum

To determine the general design response spectrum with 5% damping, two quantities, the 5% damped design spectral response acceleration at short periods, S_{DS}, and at 1-second period, S_{D1}, are determined by the following equations:

$$S_{DS} = \frac{2}{3} S_{MS}$$

$$S_{D1} = \frac{2}{3} S_{M1}$$

The general design response spectrum curve for 5% damping is shown in Figure 3-9 with the following additional guidelines:

1. For periods less than or equal to T_0, the design spectral response acceleration, S_a, is given by:

$$S_a = S_{DS} (T/T_0) + 0.4 S_{DS}$$

2. For periods greater or equal to T_0 and less than or equal to T_S, the design spectral response acceleration, S_a, is given by:

$$S_a = S_{DS}$$

3. For periods greater than T_S, the design spectral acceleration, S_a, is given as:

$$S_a = \frac{S_{D1}}{T}$$

where T is the fundamental period of the structure in seconds and T_0 and T_S are given by:

$$T_0 = \frac{0.2 S_{D1}}{S_{DS}}$$

$$T_S = S_{D1} / S_{DS}$$

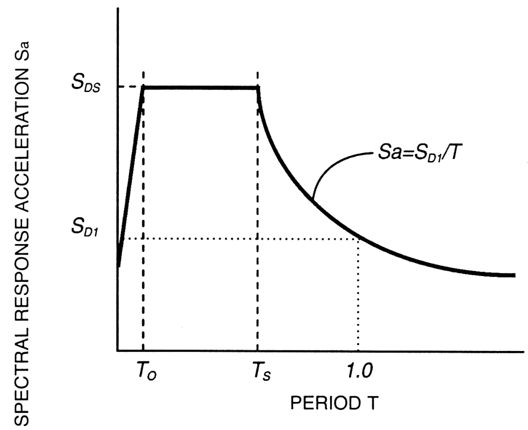

Figure 3-9. IBC Design Response Spectrum, 5% Damping (Ref. 3-10)

2000 IBC Guidelines for Site-Specific Procedure for Determining Ground Motions

The 2000 IBC Provisions requires that the site-specific study account for: the regional seismicity and geology; the expected recurrence rates and maximum magnitudes of events on known faults and source zones; the location of the site with respect to the faults and sources; near-source effects, if any; and the characteristics of the subsurface conditions. The probabilistic "Maximum Considered Earthquake" (MCE) ground motions are those represented by a 5% damped response spectrum having a 2% probability of exceedance within a 50 year period.

Because a probabilistic hazard analysis can lead to extremely high predictions of the ground motion, the 2000 IBC provides that where the probabilistic MCE spectral response ordinates at periods of 0.2 or 1.0 seconds exceed the corresponding ordinates of the deterministic maximum considered earthquake ground motion, the MCE ground motion shall be taken as the lesser of the probabilistic or the deterministic MCE ground motion. The deterministic MCE ground motion is calculated as 150% of the median spectral response accelerations (S_{aM}) at all periods resulting from a characteristic earthquake on any known active fault within the region. The MCE ground motion has a deterministic lower limit, however, as shown in Figure 3-10. The deterministic limit is determined by the site coefficients F_a and F_v that are determined as described earlier in Section 3.3.8.3, tables 3-10 and 3-11, and S_S is assumed to be 1.5g and S_1 is assumed to be 0.6g.

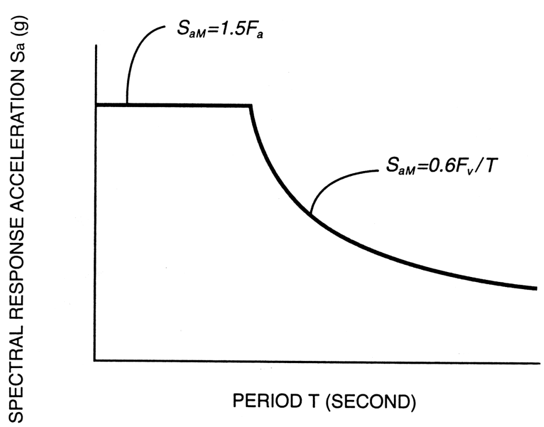

Figure 3-10. Probabilistic Ceiling on Maximum Considered Earthquake Ground Motion (Ref. 3-10)

The 2000 International Building Code has guidelines for the calculation of the deterministic MCE ground motion. The deterministic MCE ground motion is to be calculated as the spectral response accelerations (S_{aM}) at all periods resulting from a characteristic earthquake on any known fault within the region that has a slip rate exceeding 1 mm per year, using the mean-plus-one standard deviation ground motion attenuation relationship.

The design spectral response acceleration, S_a, is to be determined by:

$$S_a = \frac{2}{3} S_{aM}$$

In addition, S_a must be greater than or equal to 80 percent of the design spectral response acceleration, S_a, determined by the general response spectrum from the

The procedures in the 2000 IBC will undoubtedly be confusing until mastery of a new language and philosophy is achieved. The Near-Source factors of the 1997 UBC are replaced with a set of maps of the mapped MCE spectral response accelerations that are based on the locations of major active earthquake sources.

3.4 SOIL LIQUEFACTION

Figure 3-11. Liquefaction-induced bearing capacity failure and settlement of a five-story building in Adapazari, Turkey, most of the ground floor is below grade. Photograph courtesy of Dr. Robert May, Gibb Ltd., Reading, U.K.

3.4.1 Causes of Liquefaction

Soil liquefaction during an earthquake is a process that leads to loss of strength or stiffness of the soil. This could result in the settlement of structures, cause landslides, precipitate failures of earth dams, or cause other types of hazards. Soil liquefaction has been observed to occur most often in loose saturated sand deposits.

During strong earthquake shaking, a loose saturated sand deposit will have a tendency to compact and, thus, have a decrease in volume. If this deposit cannot drain rapidly, there will be an increase in the pore water pressure. The effective stress in the sand deposit is equal to the difference between the overburden pressure and the pore water pressure. With increasing oscillation, the pore water pressure will increase to the point where the pore water pressure will be equal to the overburden pressure. Since the shear strength of a cohesionless soil is directly proportional to the effective stress, the sand will not have any shear strength and is now in a liquefied state. "Sand boils" appearing at the ground surface during an earthquake is evidence that liquefaction has occurred.

Figure 3-12. Liquefaction-induced tilting of three-story residential structure in Central Taiwan. Photograph by Dr. Farzad Naeim.

Liquefaction can have a significant and sometimes devastating effect on buildings supported on the upper soils without consideration of the consequences of liquefaction. Figures 3-11 and 3-12 present examples of the effects of liquefaction on buildings in the 1999 Kocaeli, Turkey and Chi-Chi, Taiwan earthquakes.

3.4.2 Evaluating the Liquefaction Potential by Standard Penetration Tests

There are a number of different methods by which the potential for liquefaction of a soil can be evaluated. These methods generally compare the cyclic shear resistance of the soil with the cyclic shear stresses and strains caused by an earthquake. Simplified empirical methods have been developed that utilize case histories of past occurrences (or non-occurrences) of liquefaction during significant seismic events. Other methods use analytical techniques that incorporate dynamic analysis and laboratory testing. The most common and traditional method of analysis uses correlations between the liquefaction characteristics of soils and the Standard Penetration Test or N-value as originally described by Seed et al.[(3-11)] Since the analysis was first introduced, the methodology has been refined and various corrections are applied to account for variability in sampling and performance; a summary of recent concensus opinion on liquefaction evaluation was conducted by NCEER and has been edited by Youd and Idriss[(3-12)]; those concensus opinions are presented herein. Thus, for analysis, a corrected N-value is used. The value of the corrected N-value, denoted as $(N_1)_{60}$ is found by the formula:

$$(N_1)_{60} = N_m \cdot C_N\, C_E\, C_B\, C_R\, C_S$$

where N_m is the measured standard penetration resistance, C_N is a correction factor for overburden pressure, C_E is the correction factor for hammer energy ratio, C_B is a correction factor of borehole diameter, C_R is the correction factor for rod length, and C_S is the correction for samplers with or without liners.

The overburden pressure correction factor, C_N, may be calculated from the following formula:

$$C_N = (P_a/\sigma'_{vo})^{0.5}$$

where P_a is 100 kPa or approximately atmospheric pressure (2,089 pounds per square foot) and σ'_{vo} is the effective vertical overburden pressure at the depth of the standard penetration sample. Table 3-12 shows the suggested correction factors for the other corrections.

Table 3-12. Corrections to SPT (Ref. 3-12)

Factor	Equipment Variable	Term	Correction
Overburden Pressure		C_N	$(P_a/\sigma'_{vo})^{0.5}$
Energy Ratio	Safety Hammer Donut Hammer	C_E	0.60 to 1.17 0.45 to 1.00
Borehole Diameter	65 to 115 mm 150 mm 200 mm	C_B	1.0 1.05 1.15
Rod Length	3 to 4 m 4 to 6 m 6 to 10 m 10 to 30 m >30 m	C_R	0.75 0.85 0.95 1.0 <1.0
Sampling Method	Standard Sampler Sampler without liners	C_S	1.0 1.2

With respect to the energy ratio, ER, it is believed that the approximate historical average SPT energy for North American practice is 60% of the maximum theoretical energy achievable. The ER delivered by any particular SPT setup depends on the type of hammer and anvil in the drilling system and on the method of hammer release. The correction factor, C_E, normalizes the N-value to a 60% ER.

During an earthquake, the soils will be subject to cyclic shear stresses induced by the ground shaking. The average cyclic stress ratio (CSR) during an earthquake may be estimated by the following formula:

$$CSR = \tau_{av} / \sigma'_o = 0.65\ (a_{max} / g) \cdot (\sigma_o / \sigma'_o) \cdot r_d$$

where a_{max} = maximum acceleration at the ground surface

σ_o = total overburden pressure at depth under consideration

σ_o' = effective overburden pressure at depth under consideration

r_d = stress reduction coefficient

The range of values for the stress reduction, r_d, are shown in Figure 3-13.

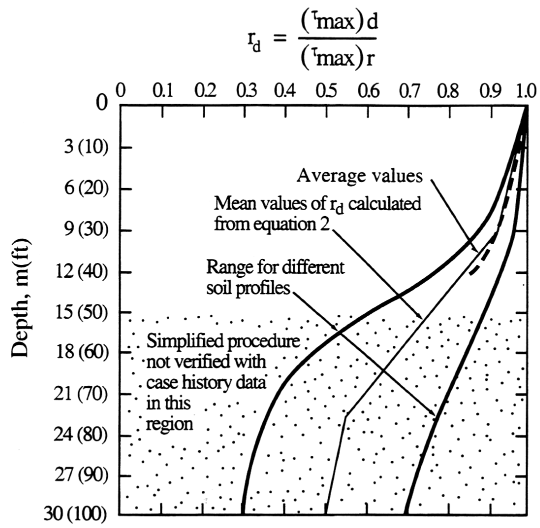

Figure 3-13. Stress Reduction Factor, r_d (Ref. 3-12)

The average value of the stress reduction coefficient, r_d, may be estimated by the following equations:

$r_d = 1.0 - 0.00765\ z$ for $z \le 9.15$ m
$r_d = 1.174 - 0.0267\ z$ for $9.15\ m < z \le 23$ m
$r_d = 0.744 - 0.008\ z$ for $23\ m < z \le 30$ m
$r_d = 0.50$ for $z > 30$ m

Having estimated the average shear stress ratio, charts similar to Figure 3-14 may be used to determine the potential for liquefaction. Figure 3-14 shows the relationship between the cyclic resistance ratio (CRR) and the corrected standard penetration resistance, N_1, for a magnitude 7.5 earthquake. The CRR is also referred to as the liquefaction resistance or liquefaction resistance ratio. If the CSR (τ_{av} / σ'_o) induced by the earthquake is less than the liquefaction resistance ratio, CRR, as shown on Figure 3-14, liquefaction would not be expected to occur; similarly if the CSR exceeds the CRR, liquefaction would be expected to occur. A factor of safety against liquefaction could be determined by the ratio of the CSR divided by the CRR. For $(N_1)_{60}$ values greater than about 30, no liquefaction would be expected and the factor of safety would be great.

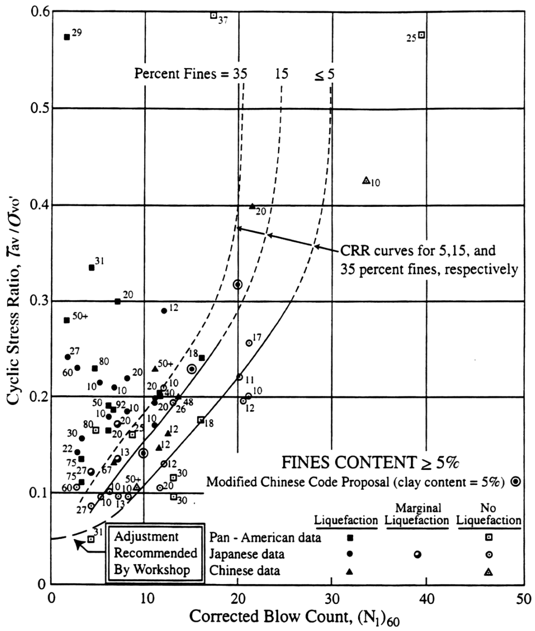

Figure 3-14. Figure 3-14. Curve Recommended for Determining CRR from SPT Data (Ref. 3-12)

The CRR base curve for clean sands (i.e., <5% fines content) may be approximated by the relationship:

$$CRR_{7.5} = \frac{a + cx + ex^2 + gx^3}{1 + bx + dx^2 + fx^3 + hx^4}$$

where:
a = 0.048
b = -0.1248
c = 0.004721
d = 0.009578
e = 0.0006136
f = -0.0003285
g = -1.673×10^{-5}
h = 3.714×10^{-6}
x = $(N_1)_{60}$

This equation is valid for values of $(N_1)_{60}$ less than 30.

Figure 3-14 also shows that the influence of the fines content on the potential for liquefaction in a way that the greater the fines content, the lesser the potential for liquefaction given the same N_1 value. I.M. Idriss and R.B. Seed have developed equations to correct the standard penetration resistance for silty sands, $(N_1)_{60}$, to an equivalent clean sand penetration resistance $(N_1)_{60cs}$. These equations are:

$$(N_1)_{60cs} = \alpha + \beta (N_1)_{60}$$

where the α and β coefficients are determined by:

$$\alpha = \exp [\ 1.76 - (190/FC^2)\ ]$$

$$\beta = [\ 0.99 + (FC^{1.5}/1000)\ ]$$

where FC is the fines content measured from laboratory gradation tests on soil samples. These equations essentially represent the CRR curves for different fines contents as shown in Figure 3-12.

As mentioned earlier, Figure 3-14 applies only for a magnitude 7.5 earthquake; to evaluate the potential for liquefaction for other magnitude events; Seed et al. (1983)[(3-13)] originally determined correlation factors that allow the induced stress ratios for other magnitude events to be adjusted to correspond to a magnitude of 7.5 by dividing the stress ratios by the factors given in Table 3-13:

Table 3-13. Seed and Idriss Original Magnitude Scaling Factors (Ref. 3-13)

Earthquake Magnitude	Magnitude Scaling Factor
5.25	1.5
6	1.32
6.75	1.13
7.5	1.0
8.5	0.89

The Seed and Idriss magnitude scaling factors are based on estimates of equivalent cycles of shear stress developed during different magnitude earthquakes. However, it is generally believed now that the original Seed and Idriss magnitude scaling factors are very conservative for moderate-sized earthquakes. Idriss has proposed a new set of magnitude scaling factors after re-evaluating the data. Idriss has proposed that the magnitude scaling factor, MSF, be defined as a function of the moment magnitude, M, as given in the equation:

$$MSF = 10^{2.24} / M^{2.56}$$

Table 3-14. Magnitude Scaling Factors Defined by Various Investigators (Ref. 3-12)

Magnitude M	Seed and Idriss (original)	Idriss	Ambreseys	Arango		Andrus & Stokoe	Youd and Noble		
							P_L<20%	P_L<32%	P_L<50%
5.5	1.43	2.20	2.86	3.00	2.20	2.80	2.86	3.42	4.44
6.0	1.32	1.76	2.20	2.00	1.65	2.10	1.93	2.35	2.92
6.5	1.19	1.44	1.69	1.60	1.40	1.60	1.34	1.66	1.99
7.0	1.08	1.19	1.30	1.25	1.10	1.25	1.00	1.2	1.39
7.5	1.00	1.00	1.00	1.00	1.00	1.00			1.00
8.0	0.94	0.84	0.67	0.75	0.85	0.8?			0.73?
8.5	0.89	0.72	0.44			0.65?			0.56?

Other researchers have also determined magnitude scaling factors; these values are shown in Table 3-14. The table also repeats the original Seed and Idriss MSF factors and also presents the new Idriss MSF factors.

There is not a concensus in the geotechnical community of which of the various sets of magnitude scaling factors to use except is it is generally accepted that the original Seed and Idriss MSF factors are conservative for magnitudes of less than 7.5. It should be noted that Arango has two sets of MSF factors. The first set was based on farthest observed liquefaction effects from the seismic energy source, estimate average peak accelerations at those distant sites, and the absorbed seismic energy requred to cause liquefaction; the second set was developed from energy concepts and the relationship developed by Seed and Idriss between numbers of significant stress cycles and earthquake magnitude. The second Arango MSF factors are similar to the new Idriss MSF factors. The Youd and Noble MSF factors are found in three sets that are a function of P_L, the probability that liquefaction did not occur.

For earthquake magnitudes greater than 7.5, it recommended that the newer Idriss MSF factors be used because it is believed that the original Seed and Idriss MSF factors were not sufficiently conservative in the upper magnitude range.

Thus, the factor of safety (FS) against liquefaction may be written in terms of the CRR, CSR and MSF factors as follows:

$FS = (CRR_{7.5}/CSR)\ MSF$

where $CRR_{7.5}$ is the cyclic resistance ratio for a magnitude 7.5 earthquake from Figure 3-14.

Example

A sand deposit has been identified beneath a site located adjacent to a river. The sand deposit is 10 feet thick and the top of the layer is 10 feet below the ground surface and overlain by a very stiff clay and is underlain by bedrock. The water level has been measured to be at a depth of 10 feet. The standard penetration resistance of the layer has been determined to be 12 blows per foot and a standard sampler was used; a drill rig with a safety hammer with an efficiency of 60% was used. The length of the drill rod is 10 meters and the borehole diameter is 5 inches (127 mm).

The design earthquake has been designated as a moment magnitude 6-3/4 event on a nearby fault and the maximum ground acceleration is expected to be 0.35 g.

The wet unit weight of the clay soils is 125 pounds per cubic foot and the wet unit weight of the sand soils is 130 pounds per cubic foot. The sands has 15% fines content according to a grain size analysis.

Compute the factor of safety against liquefaction of the sand layer.

<u>*Solution:*</u>

Step 1: Determine the effective overburden pressure at the center of the sand layer:

σ'_o = (125 pcf) (10 ft) + [(130 pcf - 62.4 pcf) (5 ft)]
= 1,588 psf

Step 2: Determine the total overburden pressure at the center of the sand layer:

σ_o = (125 pcf) (10 ft) + (130 pcf) (5 ft)
= 1,900 psf

Step 3: Determine the stress reduction factor, r_d:

z = 15 ft x (1 meter/3.2808 ft)
= 4.572 m

r_d = 1 - 0.00765 z
= 1 - 0.00765 (4.572)
= 0.965

Step 4: Determine the cyclic stress ratio, CSR.

CSR = $\tau_{av} / \sigma'_o = 0.65\ (a_{max} / g)(\sigma_o / \sigma'_o)\ r_d$
= 0.65 (0.35 g/g) (1,900 psf / 1588 psf) (0.965)
= 0.263

Step 5: Determine correction factors to SPT blowcount:

Referring to Table 3-12, the correction factors are

Overburden pressure:
C_N = $(P_a/\sigma'_{vo})^{0.5}$
= $(2{,}089 \text{ psf} / 1{,}588 \text{ psf})^{0.5}$
= 1.15

Energy ratio:
C_E = 1.0, since safety hammer is 60% efficient

Borehole diameter:
C_B = 1.0, since diameter is 5 in. (127 mm)

Rod length:
C_R= 1.0, since rod length is 10 m

Sampling method
C_S = 1.0, since standard sampler used

$(N_1)_{60}$ = $N_m \cdot C_N C_E C_B C_R C_S$
= (12) (1.15) (1.0) (1.0) (1.0) (1.0)
= 13.8

Step 6: Determine correction for fines content:

Since the fines content is greater than 5%, correction is needed.

α = exp [1.76 - $(190/FC^2)$]
= exp [1.76 - $(190/15^2)$]
= 2.50
β = [0.99 + $(FC^{1.5}/1000)$]
= [0.99 + $(15^{1.5}/1000)$]
= 1.05

$(N_1)_{60cs} = \alpha + \beta(N_1)_{60}$
= 2.50 + 1.05 (13.8)
= 17.0

Step 7: Determine the cyclic resistance ratio, $CRR_{7.5}$:

Referring to Figure 3-14, for $(N_1)_{60cs}$ = 17.0, the cyclic resistance ratio is

$CRR_{7.5}$ = 0.185

Step 8: Determine the magnitude scaling factor, MSF, for magnitude 6-3/4:

Use the Idriss magnitude scaling factor,

MSF = $10^{2.24} / M^{2.56} = 10^{2.24} / (6.75)^{2.56}$
= 1.31

Step 9: Compute the factor of safety against liquefaction:

$$FS = (CRR_{7.5}/CSR)\ MSF$$
$$= (0.185/0.263)\ 1.31$$
$$= 0.92$$

The factor of safety against liquefaction is less than unity (1.0), therefore, liquefaction would be expected to occur in the event of the design earthquake.

3.4.3 Evaluating the Liquefaction Potential by Cone Penetration Tests

Because of questions regarding the reliability and quality of the standard penetration resistances, and the inability to easily obtain a continuous profile of the resistances, there is more reliance now upon the cone penetration test (CPT). The CPT can provide a nearly continuous profile of penetration resistance and is generally more repeatable and consistent than other forms of penetration testing. One obvious deficiency of the CPT is the lack of a physical sample of the soil tested. A procedure similar to the simplified method for the SPT has been developed and is reported in the NCEER concensus document.[3-12] The chart in Figure 3-15 can be used to determine the cyclic resistance ratio ($CRR_{7.5}$) for clean sands having a fines content of less than or equal to 5% from CPT data. The chart is valid only for a magnitude 7.5 earthquake and shows the calculated cyclic stress ratio (CSR) versus the corrected normalized CPT resistance denoted as q_{c1N}. Like the chart for SPT data, the CPT chart was derived from data from sites where liquefaction effects were or were not observed following past earthquakes. The CRR curve separates the region indicative of liquefaction (above the line) from the region where there was non-liquefaction (below the line).

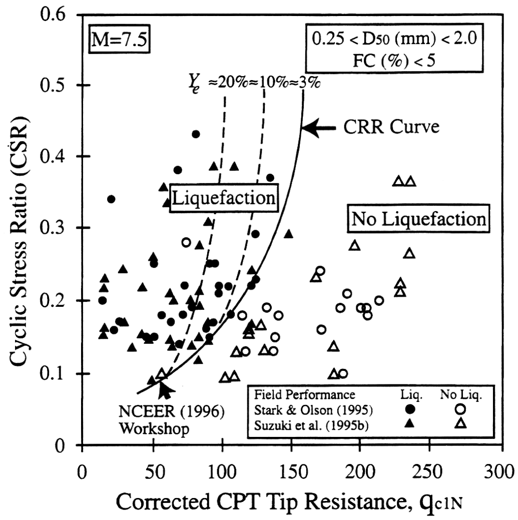

Figure 3-15. Curve Recommended for Determining CRR from CPT Data (Ref. 3-12)

The CRR curve in Figure 3-15 can be approximated by the following set of equations:

If $(q_{c1N})_{cs} < 50$

$$CRR_{7.5} = 0.833\,[(q_{c1N})_{cs} / 1000\,] + 0.05$$

If $50 \le (q_{c1N})_{cs} < 160$

$$CRR_{7.5} = 93\,[(q_{c1N})_{cs} / 1000\,]^3 + 0.08$$

where $(q_{c1N})_{cs}$ is the clean sand cone penetration resistance normalized to 100 kPa (approximately one atmosphere of pressure). The truly normalized (i.e., dimensionless) cone penetration resistance corrected for overburden stress (q_{c1N}) is given by:

$$q_{c1N} = C_Q\,(\,q_c / P_a\,) = q_{c1} / P_a$$

where:

$$C_Q = (\,P_a / \sigma'_o\,)^n$$

C_Q is the normalizing factor for cone penetration resistance; P_a is approximately one atmosphere of pressure given in the same units as the measured field CPT tip resistance, q_c, and calculated overburden pressure, σ'_o. C_Q is limited to a maximum value of 2 at shallow depths. The value of the exponent, n, is dependent on the grain characteristics of the soil. The value of n ranges from 0.5 for clean sands to 1.0 for clays. Discussion on the determination of the exponent n follows.

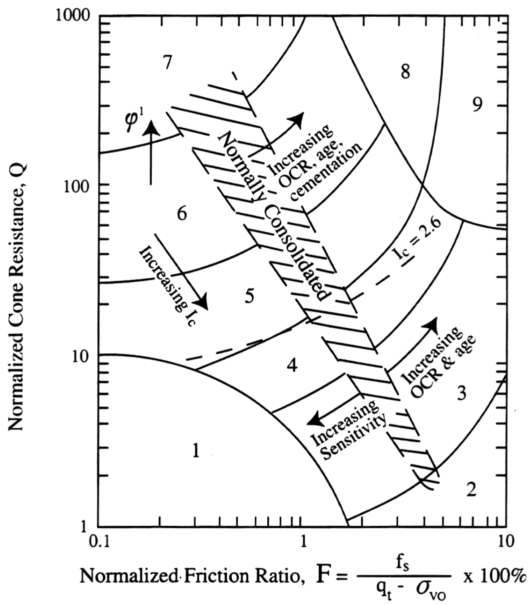

Figure 3-16. Normalized CPT Soil Behavior Type (Ref. 3-12)

Figure 3-16 can be used initially to access the soil behavior type from the CPT tests. The CPT friction ratio can be determined by taking the sleeve resistance, f_s, and dividing it by the cone tip resistance, q_c. The cone tip resistance, q_c, is determined by taking the measured tip resistance, q_t, and subtracting the total overburden pressure, σ_{vo}. The normalized cone resistance, Q, is determined by the following equation:

$$Q = [(q_c - \sigma_{vo}) / P_a]\,[(P_a / \sigma'_{vo})^n]$$

The normalized friction ratio, F, is determined by:

$$F = [f_s / (q_c - \sigma_{vo})] \times 100\%$$

The soil behavior type index, I_c, is determined by the following equation:

$$I_c = [(3.47 - \log Q)^2 + (1.22 + \log F)^2]^{0.5}$$

The soil behavior chart in Figure 3-16 was determined assuming an exponent, n, equal to 1.0, which is appropriate for clayey soils. To use the chart, the first step is to differentiate the soil types characterized as clays from the soil types characterized as sands and silts. The exponent n is assumed to 1.0 (characteristic of clays) and the dimensionless normalized CPT penetration resistance, Q, is:

$$Q = [(q_c - \sigma_{vo}) / \sigma'_{vo}]$$

If the calculated I_c using the computed Q is greater than 2.6, the soil is classified as clayey and may be too clay-rich or plastic to liquefy; verification by actual soil samples is highly recommended and checking with the so-called Chinese criteria, described later, should be done. However, if the computed I_c is less than 2.6, the soil is most likely to be granular and Q should be recomputed with the n exponent assumed to be 0.5. Now, C_Q should be calculated and the normalized CPT resistance, q_{c1N}, should be substituted for Q in the I_c calculation. If the I_c calculation gives a value of less than 2.6, the soil can be classified as non-plastic and granular. If the recalculated I_c gives a value of greater than 2.6, the soil is likely to be very silty and possibly plastic. If so, q_{c1N} should be recalculated with an intermediate value of 0.7 for n.

Finally, for sands with fines, the normalized penetration resistance, q_{c1N}, should be corrected to an equivalent clean sand value, $(q_{c1N})_{cs}$, with the following relationship:

$$(q_{c1N})_{cs} = K_c\, q_{c1N}$$

where K_c is the CPT correction factor for grain characteristics and is determined by the following equations:

For $I_c \leq 1.64, K_c = 1.0$

For $I_c > 1.64$, $K_c = -0.403\, I_c^4 + 5.581\, I_c^3 - 21.63\, I_c^2 + 33.75\, I_c - 17.88$

The appropriate values of the corrected tip resistance with the grain size correction, $(q_{c1N})_{cs}$, should then be used in Figure 3-15 to determine the $CRR_{7.5}$ and ultimately the factor of safety against liquefaction in the same manner as presented for SPT data.

3.4.4 Evaluating the Liquefaction Potential by Shear Wave Velocity

Simplified procedures have also been developed for the evaluation of liquefaction potential using shear wave velocities. However, there are some severe limitations when relying solely upon the shear wave velocities for liquefaction evaluation; these limitations include the fact that the shear wave velocities are determined in situ using low strain measurement schemes, such as seismic refraction, downhole, or crosshole surveys while the liquefaction phenomena is a large strain event. Another limitation is these seismic wave techniques do not provide a means of determining the soil type classification, particularly identifying clay soils that are non-liquefiable. The use of shear wave velocities must be accompanied by soil borings that can provide visual and laboratory confirmation of soil types.

A stress-based liquefaction procedure has been developed based on information obtained from the Imperial Valley earthquake of 1979. The normalized shear wave velocity, V_{S1}, is obtained from the field measured shear wave velocity, V_S, by the equation:

$$V_{S1} = V_S (P_a / \sigma'_{vo})^{0.25}$$

where P_a again is the reference stress of 100 kPa, approximately atmospheric pressure, and σ'_{vo} is the effective overburden pressure in units of kPa. The cyclic resistance ratio, CRR, is determined by the following equation:

$$CRR_{7.5} = a(V_{S1} /100)^2 + b (V_{S1c} - V_{S1}) - b / V_{S1c}$$

where V_{S1c} is the critical value of V_{S1} which separates contractive and dilative behavior, and a and b are curve fitting parameters which have been determined to be 0.03 and 0.9, respectively, for magnitude 7.5 earthquakes. The values of V_{S1c} depend on the fines content of sand and gravel soils and are given in Table 3-15 below:

Table 3-15. Values of Critical Shear Wave Velocity, V_{S1c} (Ref. 3-12)

Fines Content in Percent	V_{S1c} (meters/second)
<5	220
about 20	210
> 35	200

The factor of safety against liquefaction can be determined by comparing the CSR with the CRR. For earthquakes with magnitudes not equal to 7.5, the magnitude scaling factors can be used to adjust the CRR accordingly.

3.4.5 Evaluating the Liquefaction Potential by Becker Penetration Tests

Evaluation of the liquefaction potential of gravelly soils is very difficult using the standard penetration test (SPT) and the cone penetration test (CPT). The coarse size of the particles, as compared with the smaller size of the SPT sampler, can lead to high N-values that are not representative. With the CPT, the same large particles interfere with the normal deformation of soil materials around the penetrometer causing an artificial increase in the penetration resistance. To overcome these difficulties, large diameter penetrometers have been tried and one of the more effective and widely used is the Becker Penetration Test (BPT). The BPT is performed by driving a 3-meter-long double-wall casing into the ground with a double-acting diesel-driven pile hammer. The hammer impacts are applied at the top of the casing and are applied continuously. The BPT resistance is defined as the number of hammer blows required to drive the casing a distance of 300 mm. It has been recommended that the casing have an outside diameter of 168 mm; the casing should be driven by an AP-1000 drill rig with a supercharged diesel hammer and the bit should be plugged. The BPT is not used directly to estimate the liquefaction potential. The corrected Becker penetration resistance has been roughly correlated with the corrected standard penetration resistance as shown in Figure 3-17. The estimated N-values are then used to determine the liquefaction potential of the gravelly soils using the procedure for the SPT.

3.4.6 Liquefaction of Clay Soils

For clayey soils, tests performed in China have shown that certain clayey materials may be vulnerable to severe strength loss due to earthquake shaking (Seed and Idriss, Ref. 3-14). A clayey soil would be considered liquefiable if all of the following criteria are met:

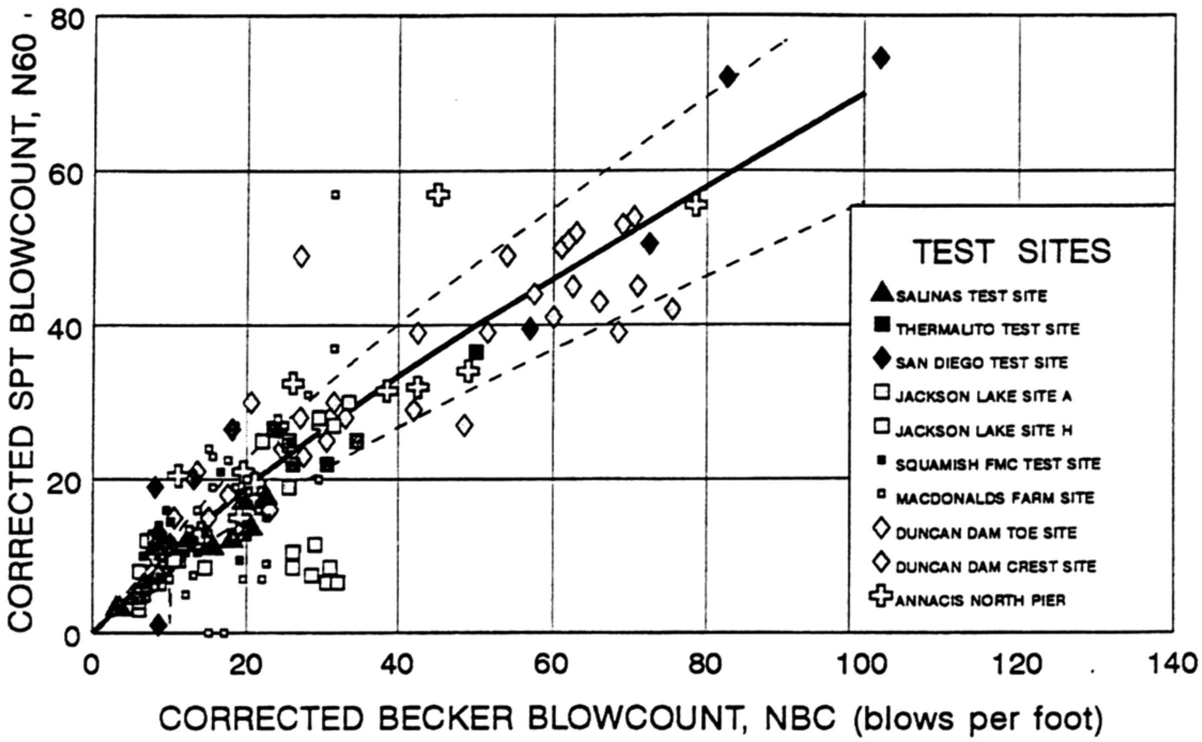

Figure 3-17. Correlation Between Corrected Becker Penetration Resistance and SPT Resistance (Ref. 3-12)

- The weight of the soil particles finer than 0.005 mm is less than 15% of the dry weight of the soil.
- The liquid limit (by Atterberg Tests) of the soil is less than 35%.
- The moisture content of the soil is less than 0.9 times the liquid limit.

Clayey soils not meeting all of these criteria may be considered to be non-liquefiable.

3.4.7 Liquefaction-Induced Settlement

When liquefaction occurs in saturated deposits, the increases in pore water pressure that cause the liquefaction to occur will eventually dissipate. This dissipation of the pore water pressure will principally be towards the ground surface; accompanying this dissipation will be some volume change of the soil deposits which will be seen at the ground level as surface settlement. Because of the generally nonhomogeneous nature of soil, these settlements will often be nonuniform and differential settlements may affect structures and lifelines. A methodology to estimate the ground settlements resulting from liquefaction of sand deposits has been proposed by Ishihara and Yoshimine[3-15]. This methodology relates the factor of safety for liquefaction to the maximum shear strain developed in a deposit and a chart was developed to determine the volumetric strain as a function of the factor of safety as shown in Figure 3-18.

Knowing the strain caused by the liquefaction, the ground surface settlement may be estimated by multiplying the thickness of each layer by the strain.

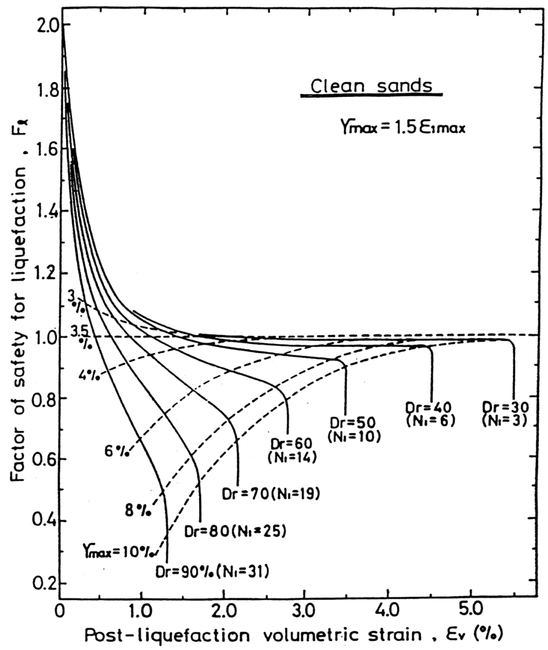

Figure 3-18. Estimation of volumetric strain based on calculated factor of safety against liquefaction as a function of relative density (Ref. 3-15)

Example

A 20 foot thick sand layer has been analyzed and found to have an induced shear stress ratio (CSR) of 0.30 while the critical shear stress ratio (CRR) was found to be 0.24. The corrected standard penetration resistance, $(N_1)_{60}$, was found to be 20. Estimate the liquefaction-induced settlement of the layer.

Solution:

Step 1: Calculate the factor of safety against liquefaction, FS:

FS = CRR / CSR
= 0.24 / 0.30
= 0.80

Step 2: Estimate the post-liquefaction volumetric strain:

Referring to Figure 3-18, using FS = 0.80 and $(N_1)_{60} = 20$,

$\varepsilon_v = 1.6\%$

Step 3: Calculate estimated settlement:

Settlement = ε_v x (Layer Thickness)
= (0.016) x (20 feet)
= 0.32 feet
= 3.84 in.

3.4.8 Liquefaction Induced Ground Failures and Effects on Structures

If a soil becomes liquefied and loses its shear strength, ground failures may result. If there are structures founded over or near these soil deposits, they may be damaged. Youd(3-16) has classified ground failures caused by liquefaction into three categories:

1) lateral spreading
2) flow failures, and
3) loss of bearing capacity.

Lateral spreading is the movement of surficial soil layers in a direction parallel to the ground surface which occurs when there is a loss of shear strength in a subsurface layer due to liquefaction. Lateral spreading usually occurs on very gentle slopes with a slope of less than six percent. If there is differential lateral spreading under a structure, there could be sufficient tensile stresses developed in the structure that it could be literally torn apart. Flexible buildings have been observed to better withstand extensional displacement than more stiff or brittle buildings(3-17).

Lateral spreading can have a very catastrophic impact upon long, linear buried utilities or, as some may prefer, "lifelines". During the great 1906 San Francisco earthquake, it is believed that every break in the water supply pipeline was caused by lateral spreading. This, of course, severely hampered fire-fighting efforts against the fires that were triggered by the earthquake which eventually destroyed much of San Francisco. Figure 3-19 shows the devastating effects of lateral spreading on a building during the 1989 Loma Prieta earthquake.

Flow failures occur when large zones of soil become liquefied or blocks of unliquefied soils flow over a layer of liquefied soils. Flow slides can develop where the slopes are generally greater than six percent. This phenomenon was tragically observed during the 1964 Alaska earthquake.

Figure 3-19. Damage to building at Moss Landing due to liquefaction-caused lateral spreading during the 1989 Loma Prieta earthquake (photograph courtesy of T.L. Youd)

Figure 3-20. Effects of Ground Oscillation in the Marina District of San Francisco as a result of the 1989 Loma Prieta earthquake.

Figure 3-21. Liquefaction-induced loss of bearing capacity of apartment buildings during the 1964 Niigata, Japan earthquake. (Photograph by the United States Geological Survey)

On flat ground, ground oscillation can occur when liquefaction at depth decouples the overlying surface layers from the underlying liquefied soil. The decoupling causes the upper surface layers to oscillate with sometimes large displacements or visible ground waves. The observed permanent displacements are usually small and show no particular orientation. Evidence of ground oscillations in the Marina District of San Francisco due to the 1989 Loma Prieta earthquake were abundant as shown in Figure 3-20.

Liquefaction can also result in the loss of bearing capacity usually accompanied by large soil deformations. Structures supported on these soils may settle, tilt, or even overturn. Buried structures have even been observed to have "floated" out of the ground. In extreme cases, where the thickness of the liquefied soils is large, tilting or overturning failures could occur, such as those observed in Niigata, Japan during the 1964 earthquake (Figure 3-21). Where the thickness of liquefied soil is thin, or where there is relatively thick non-liquefied soils overlying a liquefied soil deposit, severe tilting or overturning of structures might not occur, but differential vertical settlements could occur.

Buried structures, such as underground tanks, may be subject to excess buoyancy because of the increase in the pore water pressure associated with liquefaction. Retaining structures, such as retaining walls or port structures, could also be subjected to an increase in the lateral pressures should liquefaction occur in the adjacent soils. The formation of sink holes (when sand boils occur) may cause differential settlement or tilting of structures established on shallow foundations.

Of course, the degree that structures are affected directly or indirectly by liquefaction-caused failures will depend upon how extensive the liquefaction is. If the liquefaction occurs in a thick and horizontally extensive layer of sand, the effects on structures would be expected to be very great. If, in contrast, the liquefaction is isolated to very thin and non-continuous layers or lenses of soil, structures might have very minimal or even no noticeable damage.

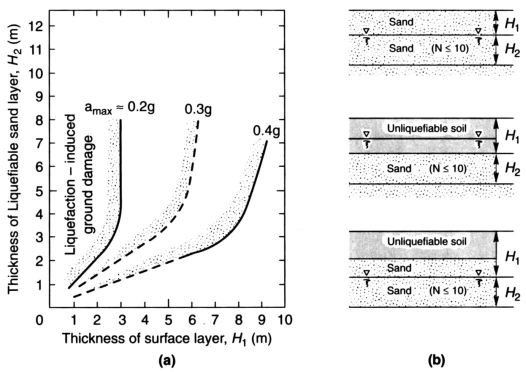

Figure 3-22. Thickness of Liquefied and Over-lying Nonliquefied Soil Layers for Determining Occurrence and Nonoccurrence of Surface Effects of Liquefaction[3-50].

Ishihara in 1985 proposed a preliminary criteria for determining the potential for disruption of the ground surface at liquefaction sites based upon empirical observations during two major Japanese earthquakes and one major Chinese earthquake.[3-18] The criteria was based upon the relationship between the thickness of the liquefiable soil layers beneath a site, and the thickness of the overlying nonliquefiable soil. Ishihara's criteria was based on ground accelerations of 200 to 250 gals, approximately 0.20 to 0.25g. The Ishihara criteria is presented in Figure 3-22. Youd and Garris[3-19] have looked further into the Ishihara's proposal and have determined that the criteria is generally correct in prediction of occurrence or nonoccurrence of surface liquefaction effects when there is no lateral spreading or ground oscillation. A methodology to estimate the magnitude of lateral spreading is presented in the following section. Determining whether ground oscillation would occur will be more subjective as to estimating whether the lateral extent of liquefiable deposit is not sufficient enough to allow for decoupling of the upper nonliquefiable soils from the lower liquefiable soils.

3.4.9 Estimating Lateral Displacement Due to Liquefaction

Several methods have been developed to estimate the lateral ground displacement at liquefaction sites. These methods include analytical models [Prevost et al., 1986[3-20]; Finn and Yogendrakumar, 1989[3-21]], physical models based upon sliding block analyses [Newmark, 1965[3-22]; Byrne et al., 1992[3-23]], and empirical models. One empirical model has been proposed by Bartlett and Youd (1992)[3-24]; They collected case history data of lateral spreading from six western United States and two Japanese earthquakes. Based on their research, they proposed two statistically independent models--one for areas near steep banks with a free face, the other for ground-slope areas with gently sloping terrain. The models are expressed in the following equations:

For free-face conditions--

$\text{Log}\ D_H = -\ 16.3658 + 1.1782\ M - 0.9275\ \text{Log}\ R - 0.0133\ R + 0.6572\ \text{Log}\ W + 0.3483\ \text{Log}\ T_{15} + 4.5270\ \text{Log}\ (100 - F_{15}) - 0.9224\ D50_{15}$

For ground slope conditions--

$\text{Log}\ D_H = -\ 15.7870 + 1.1782\ M - 0.9275\ \text{Log}\ R - 0.0133\ R + 0.4293\ \text{Log}\ S + 0.3483\ \text{Log}\ T_{15} + 4.5270\ \text{Log}\ (100 - F_{15}) - 0.9224\ D50_{15}$

Where:

D_H = Estimated lateral ground displacement in meters.

$D50_{15}$ = Average mean grain size in granular layers included in T_{15}, in mm.

F_{15} = Average fines content (fraction of sediment sample passing a No. 200 sieve) for granular layers included in T_{15}, in percent.

M = Moment magnitude of the earthquake.

R = Horizontal distance from the seismic energy source, in kilometers.

S = Ground slope, in percent.

T_{15} = Cumulative thickness of saturated granular layers with corrected blow counts, $(N_1)_{60}$, less than 15, in meters.

W = Ratio of the height (H) of the free face to the distance (L) from the base of the free face to the point in question, in percent.

Comparisons of the predicted displacements with the measured displacements in Barlett and Youd's database indicates that the predicted displacements are generally valid within a factor of 2. Bartlett and Youd comment that doubling of the predicted displacement would provide an estimate with a high probabililty of not being exceeded.

Example - Lateral Spread Displacement Near Free Face

A building is planned adjacent to a river in a highly seismic area in a foreign country. There is a steep bank at the river's edge; the bank has a height of 3 meters. The building is planned to located a distance of 7 meters from the river at its closest point. The site has a gentle uniform slope towards the river that drops 2 meters vertically over a horizontal distance of 100 meters. The ground water is at a depth of about 3 meters and is parallel to the ground surface in the direction perpendicular to the river. The geotechnical investigation performed by a local company in the foreign country provides information about the soil conditions and the report states that there is a liquefaction potential at the site.

The design earthquake is a Moment Magnitude 7.5 on a fault located 15 km from the site. The geotechnical report identifies two granular layers as being susceptible to liquefaction. The first layer is encountered between 3 and 5 meters below the ground surface; this layer has an average mean grain size of 0.33 mm, a fines content (less than No. 200 Sieve) of 15%, and a corrected Standard Penetration Blow Count, $(N_1)_{60}$, of 10. The second layer is encountered between 8 and 10 meters below the ground surface; this layer has an average mean grain size of 0.21 mm, a fines content of 35%, and a corrected $(N_1)_{60}$ value of 17.

Determine the estimated lateral displacement at the near edge of the building due to liquefaction.

<u>Solution</u>

Use the equation for free-face conditions in Section 3.4.9.

Only the upper layer needs to be included in the analysis since the $(N_1)_{60}$ value of the upper layer is less than 15 and the $(N_1)_{60}$ value of the deeper layer is greater than 15. Define parameters for analysis of the upper layer:

$D50_{15}$ = 0.33 mm
F_{15} = 15%
M = 7.5
R = 15 km
T_{15} = 5 m - 3 m = 2 m
W = H / L
= (3 m) / (7 m)
= 0.427
= 42.7%

Calculate Lateral Spread Displacement, D_H

$$\log D_H = -16.3658 + 1.1782\ M - 0.9275 \log R - 0.0133\ R + 0.6572 \log W + 0.3483 \log T_{15} + 4.5270 \log (100 - F_{15}) - 0.9224\ D50_{15}$$

$$= -16.3658 + 8.8365 - 1.0908 - 0.1995 + 1.0715 + 0.1048 + 8.7345 - 0.3044$$

$$= 0.7868$$

Then,

$$D_H = 6.1207 \text{ m}$$

Practically speaking, the lateral displacement could range from one-half to twice this estimate. Therefore, the range is:

D_H= about 3 to 12 m

Example - Lateral Spread Displacement For A Sloping Site

A power plant is to be located in an alluvial valley which has a shallow groundwater table. The site has a gentle uniform slope which drops 0.4 meters vertically over a horizontal distance 50 meters. The ground water is at a depth of about 2 meters. The geotechnical investigation provides information about the soil conditions and the report states that there is a liquefaction potential at the site.

The design earthquake is a Moment Magnitude 6.5 on a fault located 5 km from the site. The geotechnical report identifies two granular layers as being susceptible to liquefaction. The first layer is encountered between 2 and 3 meters below the ground surface; this layer has an average mean grain size of 0.25 mm, a fines content (less than No. 200 Sieve) of 45%, and a corrected Standard Penetration Blow Count, $(N_1)_{60}$, of 6. The second layer is encountered between 5 and 10 meters below the ground surface; this layer has an average mean grain size of 0.11 mm, a fines content of 35%, and a corrected $(N_1)_{60}$ value of 10.

Determine the estimated lateral displacement at the power plant site due to liquefaction.

<u>Solution:</u>

Use the equation for ground slope conditions in Section 3.5.

Determine the ground slope, S

S = V/H = (0.4 meters) / (50 meters) = 0.8 %

Both layers need to be included in the analysis since the $(N_1)_{60}$ value of the both layers is less than 15. Define parameters for analysis:

Use weighted averages:

$D50_{15}$ = [(0.25 mm) x (1 m) + (0.11 mm) x (5 m)] / [1 m + 5 m]
= 0.1333 mm
F_{15} = [(45%) x (1 m) + (35%) x (5 m)] / [1 m + 5 m]
= 36.67%
M = 6.5
R = 5 km
T_{15} = 1 m + 5 m
= 6 m

Calculate Lateral Spread Displacement, D_H

$\log D_H$ = -15.7870 + 1.1782 M - 0.9275 log R - 0.0133 R + 0.4293 log S + 0.3483 log T_{15} + 4.5270 log (100 - F_{15}) - 0.9224 $D50_{15}$
= -15.7870 + 7.6583 - 0.6483 - 0.0665 - 0.0416
+ 0.2710 + 8.1560 - 0.1230

= -0.5811

Then,
D_H = 0.2624 m

Practically speaking, the lateral displacement could range from one-half to twice this estimate. Therefore, the range is:

D_H = about 0.13 to 0.52 m

3.4.10 Facing the Liquefaction Problem

If liquefaction is identified as a hazard that could affect a structure, there are choices that must be made. For new construction, the available choices are:

1. design for liquefaction by modifying the site soil conditions or strengthening the structure.
2. abandon or move the project, or
3. accept the risks by proceeding without designing for liquefaction.

Obviously, economics will influence the selection process in a major way. The second choice would be dependent on whether there was an alternative site without the liquefaction problem. The third choice could invite unwanted liability exposure and problems of uninsurability or even jeopardize future property values and viability of the project. The second and third choices could be the subject of much discourse but is outside the intention and scope of this work and emphasis will be put upon designing for liquefaction.

3.4.11 Mitigation of Liquefaction Hazard by Site Modification

There are site modification methods which are intended to reduce the potential or susceptibility of the soils beneath a site to liquefy[(3-25)]. These methods are summarized below:

1. Excavation and replacement of liquefiable soils
   - A. Excavation and engineered compaction of the existing soil
   - B. Excavation and engineered compaction of existing soils with additives
   - C. Excavation of existing soils and replacement with properly compacted nonliquefiable soils
2. Densification of in-situ soils
   - A. Compaction piles
   - B. Vibratory probes
   - C. Vibroflotation
   - D. Compaction grouting
   - E. Dynamic compaction or impact densification
3. In-situ improvements of soils by alteration
   - A. Mixing soils in-situ with additives
   - B. Removing in-situ soils by jetting and replacement with nonliquefiable soils
4. Grouting or chemical stabilization

Excavation and Replacement of Liquefiable Soils. The first general category of site modification methods involves the excavation of the potentially liquefiable soils. This soil may then be recompacted as an engineered fill to a higher density so that the soil will have less potential to liquefy. Alternatively, the native soils may be improved with some additives and then properly compacted as an engineered fill. Another solution would be to waste the excavated material and replace it completely with properly compacted import material that would be nonliquefiable. As the liquefiable soils will most likely be below the water table, dewatering will be needed and excavation could be difficult due to high moisture content of the soils; these two factors may make recompaction less desirable and uneconomical.

In-Situ Densification. The second general category of site improvement methods is in-situ densification of the liquefiable soils. By densification, the soils would have less potential to liquefy because a more dense soil would not tend to have a decrease in volume when subjected to earthquake shaking; instead, a more dense soil would have a tendency to become less dense thus reducing the possibility of excess pore pressures developing.

The driving of piling into ground will produce both vibrations and displacement in the soils which would lead to densification and increased soil strength. It would be more beneficial to drive piling that would have a significant cross sectional area to maximize the lateral displacement of the soils; thus a solid pile such as a timber, concrete, or closed-end pipe pile section would be much more effective than an H-section pile. Another form of compaction piling (or displacement piles) is a sand filled steel pipe that is withdrawn after driving; the pile is pulled increments of about 6 feet and the hole is backfilled with sand. The pile is then redriven to compact the sand and this process is repeated until the steel pile is completely withdrawn; this allows the steel pile to be reused. Compaction piles have reportedly been used to stabilize hydraulic fill consisting of sand beneath a building at Treasure Island in San Francisco Bay [(3-26)]; liquefaction of the treated soils did not occur in the 1989 Loma Prieta earthquake whereas liquefaction was observed in non-treated areas at other parts of Treasure Island.

Vibratory probes describes methods commonly referred to as “vibro systems or techniques." Vibro systems are probably the most commonly used countermeasure among all of the mitigation techniques available [(3-27)]. The vibrator is 12 to 18 inches in diameter and about 10 to 16 feet in length. Rotating eccentric weights mounted on a casing above the probe produce vibrations close to the tip of the probe.

Vibroflotation is one such proprietary vibro process by which a machine is lowered into the ground and compacts loose soils by simultaneous vibration and saturation [(3-28)]. As the machine vibrates, water is pumped in faster than it can be absorbed by the soil. The more granular particles are vibrated in a more dense state while the excess water carries off the finer particles to the ground surface (see Figures 3-23 and 3-24). Granular soils are added from the ground surface to compensate for the loss of the finer particles and the increased density. It has been reported by Ishihara et al.[(3-29)] that oil tanks supported on sand soils compacted by the Vibroflotation technique suffered little damage and settlement in the 1978 Miyagiken-Oki earthquake in Japan, while nearby similar facilities supported on loose sand deposits that were not densified suffered considerable damage and significant settlement. Vibro compaction is a similar process although the use of water jets may not be used. Vibro compaction is generally effective in clean sand soils having less than 10% fines content (passing the No. 200 sieve). Where the fines content of sands is greater than 10%, or where there may be sands interbedded with cohesive layers, vibro replacement or "stone columns" would be viable; this method is described in more detail later in this section.

Another method of in-situ densification is compaction grouting. Grout pipes are typically installed by driving or by drilling and inserting steel pipes through which low slump, mortar-type grout is pumped under high pressure to densify loose soils[(3-26)].

In-situ densification may also be accomplished by dynamic compaction (which is also referred to as impact densification or heavy tamping). Dynamic compaction is a method which utilizes a heavy falling weight to produce a shock wave which is propagated to some depth in the ground (Fig. 3-25).

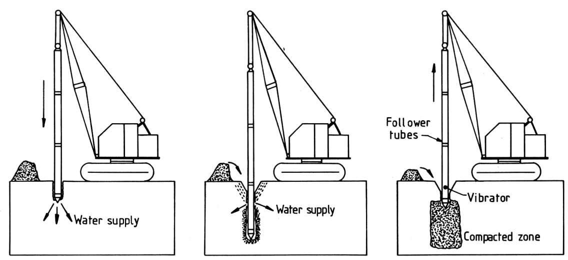

Figure 3-23. Vibroflotation technique. (Illustration courtesy of Hayward Baker, Inc.)

Figure 3-24. Water being pumped during vibroflotation. (Photograph courtesy of Hayward Baker, Inc.)

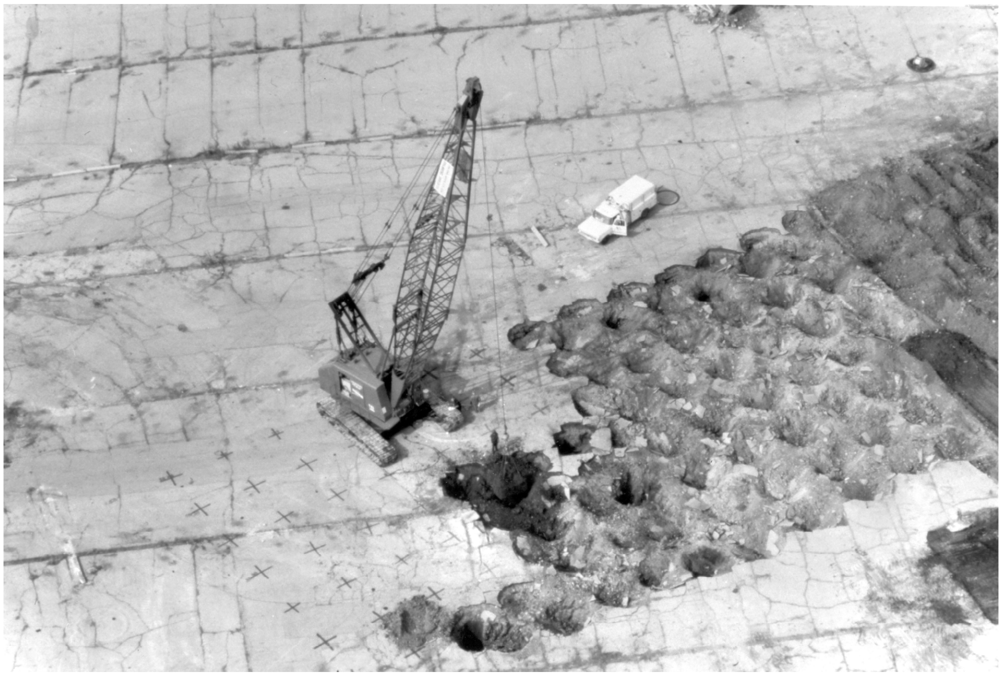

Figure 3-25. Dynamic Compaction technique. (Photograph courtesy of Hayward Baker, Inc.)

The effect of this compaction in granular soils is to generate high pore water pressures. As these high pore water pressures are dissipated by drainage, compaction (or more correctly, consolidation) occurs and the soils become more dense and, therefore, more resistant to liquefaction. In the United States, it is typical to use weights ranging from 10 to 35 tons that are dropped from heights of 50 to 120 feet. The energy is controlled by selection of the weight, drop height, the number of drops at each point and the spacing of the grid of drop points. The effective depth of treatment has been empirically estimated as shown in Figure 3-26; this figure shows the effective depth of treatment (in meters) as a function of the metric energy input expression of $(WH)^{0.5}$, where W is the weight to be dropped in tonnes and H is the drop height in meters [3-30]. The effective depth of treatment has also been expressed in the form of the equation:

$$D = N\,(WH)^{0.5}$$

where N is a number between 0.3 and 0.7 depending on the material to be densified.

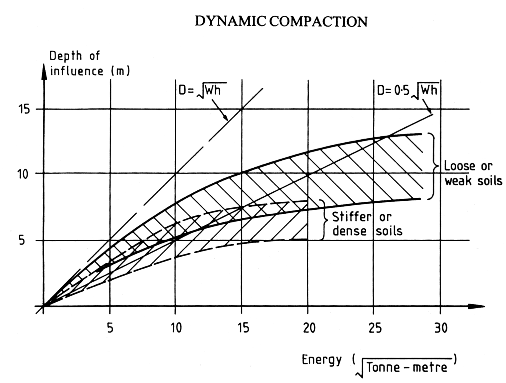

Figure 3-26. Chart to determine effective depth of treatment by Dynamic Compaction.(Ref. 3-30)

In-situ densification could also be accomplished by deep blasting. This method would use small explosive devices installed at depth to densify loose sandy materials.

Soil Alteration. The third major category of soil improvement methods is alteration of the soil to reduce the potential for liquefaction. The soil may be made more resistant by the construction of mixed-in-place solidified piles or walls. Lime, cement, or asphalt may be mixed-in-place to create piles or walls to provide shear resistance which would confine an area of liquefiable soils to prevent flow.

Vibro-replacement is a process by which soils can be improved and is especially suitable when there are significant amounts of fine soils which do not readily respond to vibratory compaction. With vibro-replacement, a vibrator is used to penetrate the soil to a desired depth and the resulting cavity is filled with coarse-grained material which may consist of stone. This material is then compacted and forms a "stone column" (see Figure 3-27). The stone provides better transmission of the vibratory forces to the surrounding soils and therefore provides better densification. Stone columns would be installed on a pre-determined grid pattern. The stone columns would have a low compressibility and high shear strength. Because of its coarse-grained nature, excess pore pressures developed during an earthquake in the surrounding soils can be quickly dissipated.

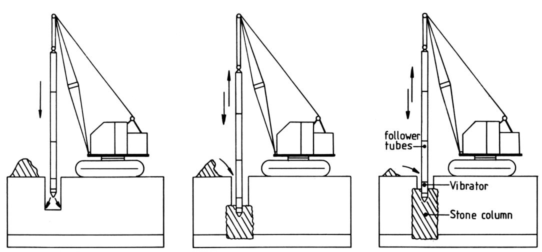

Figure 3-27. Vibro-Replacement technique. (Illustration courtesy of Hayward Baker, Inc.)

Grouting or Chemical Stabilization. The fourth category of soil improvement methods is soil grouting or chemical stabilization. These methods would improve the shear resistance of the soils by injection of particulate matter, resins, or chemicals into the voids. Common applications are jet grouting and deep soil mixing [(3-27)].

Jet grouting is a system where cylindrical or panel shapes of hardened soils are created to replace potentially liquefiable soils. A specially manufactured drill is used that has high pressure side jetting nozzles to cut and lift the soil to the surface while simultaneously injecting grout. The resulting mixture is commonly called "soilcrete."

Deep soil mixing is a technique that uses hollow stem auger drilling equipment with paddles to mix cementitious materials into the soils to create a "soilcrete" or similar mixture [(3-27)]. Gangs of 2 to 5 shafts with hollow stem augers are used. The augers could be up to 40 inches in diameter and could mix soils to depths of up to 200 feet [(3-31)]. Each auger is a discontinuous auger shaft that has mixing paddles. The augers drill into the soils and grout is pumped through the hollow stems and injected into the soil at the tip. Deep soil mixed walls are created with this process as the augers are used in tangent configurations. The use of deep soil mixing in liquefaction stabilization may involve the construction of a perimeter soil-cement cutoff wall installed to isolate loose cohesionless soils beneath a structure. The groundwater could be lowered to provide a dry or nonliquefiable zone beneath the structure. Reinforcement of liquefiable soils can be accomplished by the soil-cement walls in a block or lattice pattern to resist the stresses from embankments or other structures when loose cohesionless foundation materials liquefy as a result of an earthquake. This method of soil reinforcement was used to stabilize the Jackson Lake Dam in Wyoming [(3-32)] and a site in Kagoshima City, in western Japan for a 3-story building [(3-33)].

3.4.12 Mitigation of Liquefaction Hazard by Structural Design

Designing a structure to resist liquefaction must take into account the deformations of the soil that could occur in the event of liquefaction occurrence. This will greatly effect the foundation design of the building.

Designing for liquefaction may be accomplished by the use of piles or caissons which rely upon the soil or rock beneath the potentially liquefiable soil layers for support. These designs would need to account for possible downdrag forces that would develop on the piles or caissons because of the settlement of the upper soils that could occur. Also, special design for the lateral forces or base shear may be needed because there could be a significant loss of the ability to transfer horizontal forces to the liquefied soils; this may require the use of battered piles or the design of caissons as unsupported columns through the liquefied zones. However, the use of battered piles is being discouraged because of the rigid connections the piles have with the pile caps. Under seismic excitation and liquefaction, these connections may be subjected to bending moments that could result in severe damage to the piles and/or the pile caps. Extensive damage to battered piles supporting wharf structures was observed in the Port of Oakland as a result of the 1989 Loma Prieta earthquake.

Because of the possibility of lateral spreading, the foundation system will need to be tied together quite well to act as a single unit. Floor slabs on grade could be subject to settlement or differential movement and may need to be structurally supported.

For structures of relatively low profile and relatively uniform mass distribution, a mat foundation may be feasible. The mat would be able to bridge the local areas of settlement and the structure should be able to act more or less as a rigid body. Any permanent deformations of the structure could be corrected by injection grouting or mud-jacking the structure to its proper level.

Wall structures retaining potentially liquefiable soils, such as those that might be found at port and harbor facilities, may be subjected to greater than normal lateral earth and hydrostatic pressures should liquefaction occur. Earth pressures could increase from an at-rest or active earth pressure condition to a condition where the pressure distribution could be equivalent to that imposed by a fluid having a density equal to the total unit weight of the soil.

With a structural solution to mitigate against liquefaction, there will remain a significant risk that some damage could occur to the structure and that almost certain remedial and corrective work will be likely after the liquefaction event.

3.4.13 Mitigation of Liquefaction Hazard by Drainage

Dewatering systems may reduce the potential for liquefaction by removing the water from those layers which could liquefy. Also, the increase in effective overburden pressure will add to the resistance of the soils against liquefaction. If total dewatering of a site is not practical, providing some means of drainage may mitigate the problem. Drainage solutions to mitigate liquefaction allow for the rapid dissipation of excess pore pressures in the potentially liquefiable soil layers. If the pore pressures can be relieved quickly, the effective stresses will not decrease significantly and the soil will retain most of its shear strength not allowing liquefaction to occur. Vertical gravel drains placed in a grid pattern may be able to accomplish this. Vibro-replacement also utilizes this principle as part of its mechanism to mitigate liquefaction as the coarse-grained stone columns would be very permeable in comparison to the surrounding soils.

There are methods under development to utilize prefabricated drainage material similar to conventional vertical wick drains to control the effects of liquefaction. These drains would be of sufficient size to accommodate the large volumes of water generated during a liquefaction event without undue head loss. An integral water reservoir allows water to be stored during an earthquake; the water is gradually drained back into the surrounding soils. A water outlet would not be required for this system.

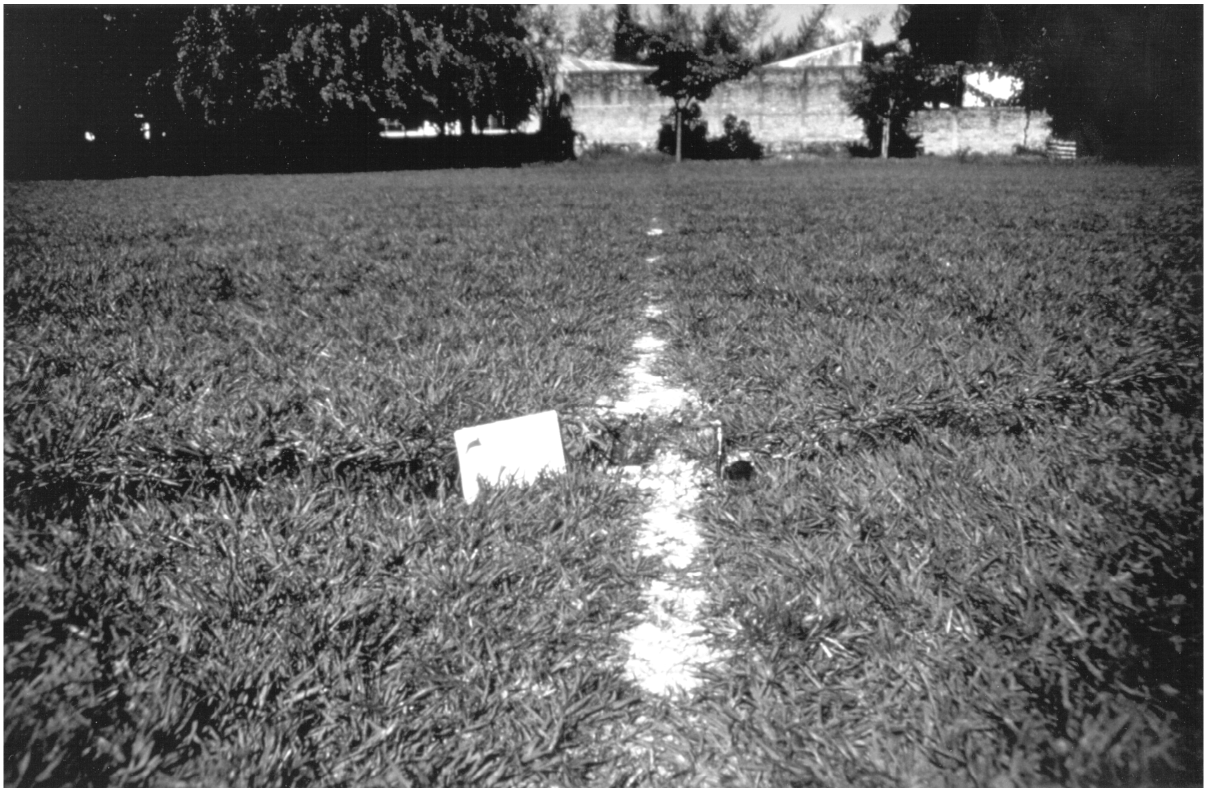

Figure 3-28. Differential compaction between an area with older natural soils and an area with loose fill soils from the 1986 San Salvador earthquake. (Photograph courtesy of Mr. Robert Chieruzzi)

3.5 SEISMIC SETTLEMENT, SUBSIDENCE AND DIFFERENTIAL COMPACTION

Seismic settlement and subsidence are two terms used to describe surface subsidence which is a result of compaction or densification of granular soils from earthquake-induced vibrations, which may occur over large areas. Although this phenomenon produces a result which is similar to what occurs from liquefaction, it occurs in dry or partially saturated soils or in saturated soils which have good drainage, that is, those soils that do not liquefy[(3-34)].

During an earthquake, a granular soil is subjected to cyclical shear from horizontal and vertical accelerations. In a strong earthquake, the horizontal motions can cause densification because of the numerous shear cycles that occur. Whitman and DePablo have suggested that vertical accelerations greater than 1 g (g = acceleration of gravity) are required to cause significant densification of granular soils. [(3-35)] However, it has been reported that over one meter (about three feet) of ground subsidence due to densification was experienced in Valdivia, Chile during the 1960 earthquake [(3-36)]. It has also been reported that there was ground subsidence in the order of 5 to 7 meters over a very large area in the Mississippi Valley as a result of the New Madrid earthquakes of 1811 and 1812 [(3-34)]. It is difficult to determine whether some of these reported instances of subsidence were at least partially due to liquefaction or some tectonic movement, or if they were totally a result of seismic settlement.

Differential compaction occurs when there is marked difference in the density of the soils in a horizontal sense. Such a phenomena was observed during the San Salvador Earthquake of 1986 (Figure 3-28).

Tokimatsu and Seed have proposed a simplified procedure to estimate the settlement of dry sands due to earthquake shaking without having to perform a dynamic response analysis.[3-37] They claim that the primary factor controlling settlements in dry sands is the cyclic shear strain induced in the soils at various depths. At any given depth, the effective shear strain, γ_{eff}, may be estimated by the relationship:

$$\gamma_{eff} = \tau_{av} / G_{eff} = [\ \tau_{av} / G_{max}\ ] / [\ G_{eff} / G_{max}\ ]$$

where G_{max} is the shear modulus at low strain level, G_{eff} is the effective shear modulus at the induced strain level, and τ_{av} is the average cyclic shear stress at the corresponding depth. τ_{av} may be computed by the following equation:

$$\tau_{av} = 0.65\ (a_{max} / g) \cdot \sigma_o \cdot r_d$$

Substituting this into the earlier equation and rearranging the terms, we get the following equation:

$$\gamma_{eff}\ [\ G_{eff} / G_{max}\ ] = 0.65\ (a_{max} / g) \cdot \sigma_o\ r_d / G_{max}$$

The right-hand side of the equation can be evaluated for any depth. G_{max} may be evaluated by the relationship developed by Seed and Idriss[3-38] given below:

$$G_{max} = 1{,}000 \cdot (K_2)_{max} \cdot (\sigma'_m)^{1/2}$$

in units of pounds per square foot

where $(K_2)_{max}$ is approximately equal to 20 $(N_1)^{1/3}$ and σ'_m represents the median effective stress on the soil at the given depth. Having computed the value of γ_{eff} [G_{eff} / G_{max}], Figure 3-29 may be used to determine the effective shear strain, γ_{eff} . Knowing the effective cyclic shear strain, the volumetric strain, ε_c , can be estimated by the use of Figure 3-31 which relates the strains for different N_1 values for a given 15 equivalent uniform strain cycles, which are representative of a magnitude 7.5 earthquake.

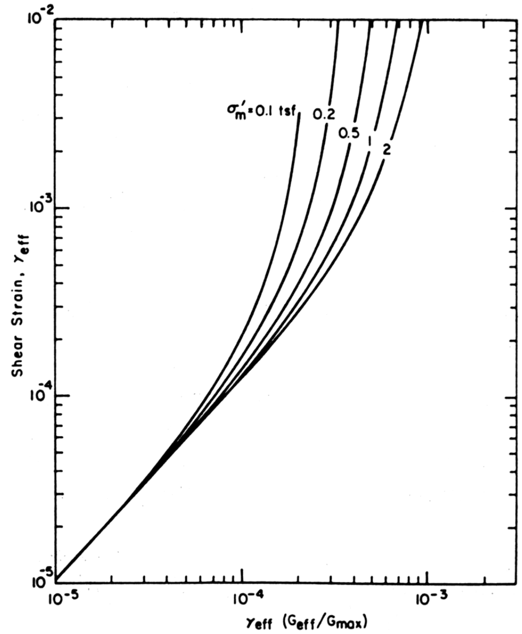

Figure 3-29. Plot for determination of induced shear strain in sand deposits (Ref. 3-37)

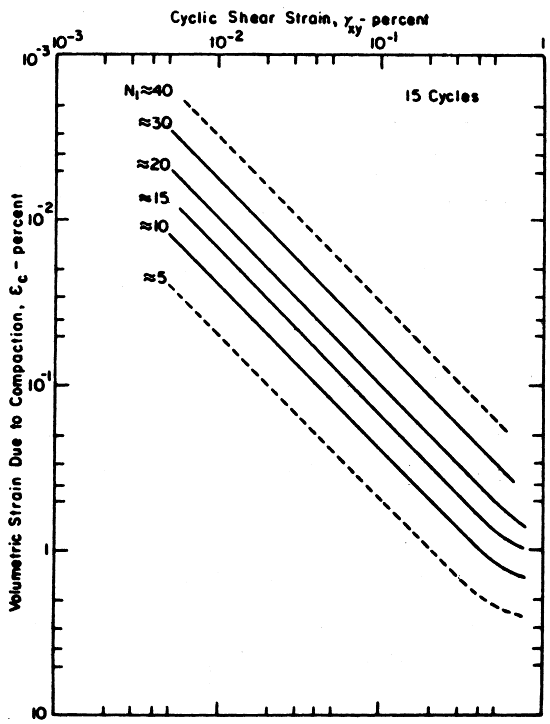

Figure 3-30. Relationship between Volumetric Strain, Shear Strain, and Penetration Resistance for dry sands (Ref. 3-37)

Figure 3-31. The Turnagain Heights landslide occurred as a result of the 1964 Great Alaska earthquake and had length of about 1.5 mi. and width from 1/4 to 1/2 mi. (Photograph by United States Geological Survey)

To account for earthquakes of different magnitudes, Seed and Tokimatsu have proposed the following Table 3-16 which relates the number of representative cycles of cyclic shear strain to different earthquake magnitudes to provide a correction factor.

Table 3-16. Correction Factors for Different Magnitude Earthquakes (Ref. 3-37)

Earthquake Magnitude	Number of representative cycles at 0.65 τ_{max}	Volumetric strain ratio $\varepsilon_{c,N} / \varepsilon_{c,N=15}$
8-1/2	26	1.25
7-1/2	15	1.0
6-3/4	10	0.85
6	5	0.6
5-1/4	2-3	0.4

Because the results in Figure 3-30 are based on tests that were performed under unidirectional simple shear conditions, Seed and Tokimatsu recommend that the estimated volumetric strain be doubled to account for multidirectional effects of earthquake shaking. The amount of dry settlement due to earthquake shaking may then be obtained by multiplying the corrected volumetric strain by the thickness of the sand layer.

3.6 LANDSLIDING AND LURCHING

3.6.1 Landsliding

Earthquakes may trigger landslides or other forms of slope instability. Slope failures may occur as a result of the development of excess pore pressures which will reduce the shear strength of the soils or cause loss of strength along bedding or joints in rock materials. The Turnagain Heights landslide occurred as a

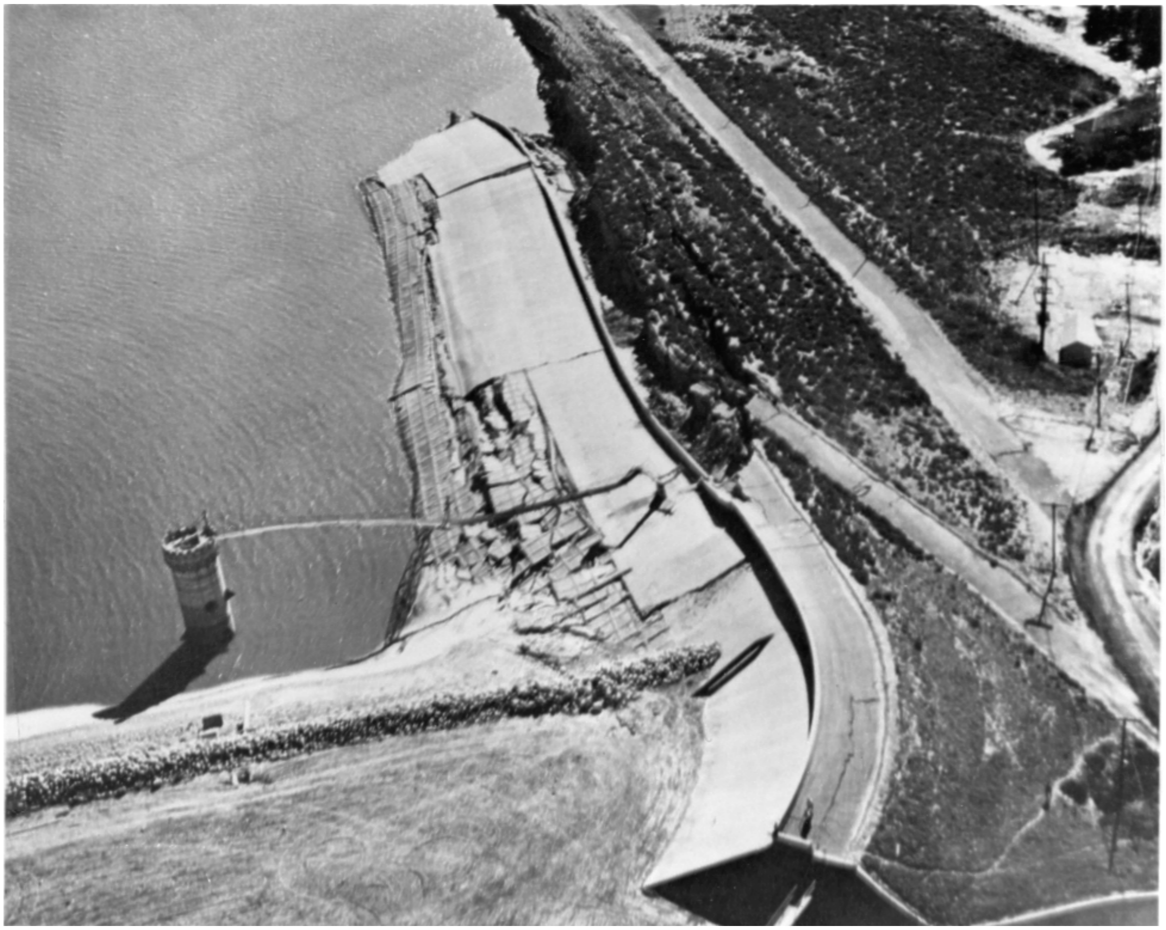

Figure 3-32. Lower Van Norman Dam after the 1971 San Fernando earthquake. (Photograph by the United States Geological Survey)

result of the 1964 Alaska earthquake (Fig. 3-31). The epicenter of the Richter magnitude 8.5 earthquake was about 130 kilometers from Anchorage but the duration of strong ground motion lasted more than three minutes. Seed and Wilson believe that the long duration of the ground motion caused the pore water pressures to continually increase causing liquefaction of silt and fine sand lenses which led to the landslide.[3-39] Earthquake-caused liquefaction within the Lower Van Norman Dam during the February 9, 1971 San Fernando earthquake nearly resulted in the overtopping of the dam (see Figure 3-32) which would have threatened tens or hundreds of thousands of people who lived beneath the dam in the densely populated San Fernando Valley.

Earthquakes may also cause shallow debris slides in areas with high, steep slopes. These slides could be quite minor or quite major, such as the 1970 debris avalanche triggered by the Peruvian earthquake of May 31, 1970 which buried the towns of Yungay and Ranrahirca in which 18,000 lives were lost.

Careful consideration should be given to structures that are sited in a location that could directly or indirectly be affected by some form of slope instability. A very careful geotechnical and geologic investigation would be needed to identify if such hazards exist and determine if there are any practical means of mitigation of the hazards.

3.6.2 Lurching

Lurching is a phenomena where there is movement of soil or rock masses at right angles to a cliff or steep slope. Structures founded either in part or whole on such masses may experience significant lateral and vertical deformations.

3.7 FLOODING, TSUNAMIS AND SEICHES

3.7.1 Flooding

Seismic activities may cause some calamity elsewhere which could result in flooding at the site under consideration. An important part of the site investigation should include the identification of any bodies of water or structures that contain water that are located above or upstream of the site. The consequences of failure of these bodies or structures should be evaluated to determine what are the probable flood limits and depths of inundation that could be expected. The impact of this potential flooding on structure and function could have an effect on the siting of a building. It may be practical to raise the finished floor elevation to be reasonably above the maximum expected flood elevation; if this is not possible, re-siting of the proposed building may be necessary. Otherwise, emergency procedures will need to be established in the event that the flood hazard becomes a reality.

In some regions of the United States, studies of flood hazard have been performed and flood maps are available. Some of these studies have been performed by the United States Army Corps of Engineers; others are available from the Federal Emergency Management Agency (FEMA).

3.7.2 Tsunamis

A tsunami is a long sea wave that could be generated by a rapidly occurring change in seafloor topography caused by tectonic displacement. Such tectonic displacements may be caused by earthquakes, undersea landslides or volcanic eruptions. It is believed that strike-slip earthquakes are less likely to cause tsunamis and that a substantial vertical offset caused by a dip-slip earthquake mechanism is necessary to generate large tsunamis. A tsunami may be caused by a nearby fault rupture, or by distant earthquakes which may be thousands of miles away. In the open sea, these waves travel at great velocities, however, the amplitudes of these waves are quite small with a very long wavelength. The velocity of a tsunami water wave is approximately given by the relationship

$$v = (gD)^{0.5}$$

where g is the acceleration of gravity and D is the water depth. As the wave approaches a coastline, the shallower depth of water will cause the amplitude of the water wave to become greater. The wave may become even more accentuated where there are topographic features such as narrow bays and very shallow waters. In fact, the meaning of the word tsunami is literally "harbor wave" in the Japanese language. The wavefront may crash on shore and may extend its damaging influence inland.

Tsunamis do not occur with every earthquake with its source beneath the seafloor. Although tsunamis do not occur that often, they can cause significant damage and loss of life. Tsunamis have occurred most frequently in the Pacific Ocean. Japan has been the victim of numerous tsunamis throughout recorded history. The city of Hilo on the big island of Hawaii has been devastated several times by tsunamis; the offshore topography is conducive to channeling the destructive forces of a tsunami into waves that were estimated to be from 21 to 26 feet high in the 1946 tsunami. Great damage from tsunamis occurred as a result of the so-called Great Alaska Earthquake of March 27, 1964 (see Figures 3-33 and 3-34). Although not as frequent, tsunamis have also

Figure 3-33. Waterfront at Seward, Alaska, looking south, before the 1964 Great Alaska earthquake generated underwater landslides, surge waves, and tsunami waves that devastated the waterfront. (Photograph by United States Geological Survey)

Figure 3-34. Waterfront at Seward a few months after the earthquake, looking north. (Photograph by United States Geological Survey)

occurred in the Atlantic and Indian Oceans. Tsunamis have even been reported in the Mediterranean Sea [3-34; 3-40].

Structural damage from tsunamis is caused by the force of the water and the impact from boats and any other objects that may be carried and propelled by the moving waters. Structures with open fronts or large areas of glass with continuous rear walls were found to have a greater potential to be damaged. Observations made after several tsunamis suggest that light frame buildings are subject to very severe damage or total destruction because of the relatively flexible type of construction. Heavy timber construction is also found to be very susceptible to damage from tsunamis. If not firmly anchored to the foundations, such structures would have a tendency to float if the water level was significant. Heavier buildings constructed of structural steel or reinforced concrete tend to be less damaged. Although structures have been observed to have withstood tsunami forces, the structural elements at the lower levels could sustain significant damage from the passage of the water and impact by objects.

It has been suggested that a structure could be designed to resist tsunami waves.[3-41] Special consideration would be needed to minimize the effects of a tsunami. First, the major axis or long dimension of the building should be oriented parallel to the expected direction of the wave. A building with this orientation would have a minimal surface area that could be attacked by the on-coming waves. In addition, the building will have greater strength to resist the wave forces because of the greater amount of structural elements providing resistance along the major axis. Consideration should also be given to leaving the lower portion of the building completely open which would greatly reduce the total load applied to the structure from the tsunami wave.

The forces exerted on a structure by a tsunami are not easy to predict. The horizontal fluid pressure exerted by flowing waters, p, can be estimated by the equation

$$p = 0.5\, C_D\, \rho\, V_S^2$$

where C_D is a coefficient of drag for submerged objects which is a function of the shape of the object (which may be a wall or a column), ρ is the mass density of water, and V_S is the speed of the water surge which is approximated by

$$V_S = 2\,(g\, d_s)^{0.5}$$

where g is the acceleration of gravity and d_S is the height of the water surge [3-41]. In addition to the dynamic fluid pressures, there could be impact loading from objects carried by the tsunamis.

3.7.3 Seiches

A seiche may occur when earthquake ground motion causes water in closed or partially closed body (such as a bay, lake, reservoir, or even a swimming pool) to oscillate from one side to the other[3-34] . Large seiches may occur when the frequency of the in-coming earthquake waves are the same as the natural frequency of the water body and causes resonant oscillation. This oscillation could cause overtopping of dams and damage to structures located near the water, and could continue for hours.

3.8 SOIL-STRUCTURE INTERACTION

3.8.1 Conventional Structural Dynamic Analysis and Soil-Structure Interaction

In the normal dynamic analysis of a building, the usual method of dynamic analysis is to determine the free field ground motion at the site of the building, and to apply that free field ground motion at the base of the building assuming that the base is fixed. This may be true for the case where the building is founded on rock. However, if the building is founded on soft soils, the earthquake motion at the base of the building is not likely to be identical to the free field ground motion. The presence of the structure will modify the free field motions because the soil and structure will interact to create a dynamic system quite different from just a free field condition. This "soil-structure interaction" will result in a structural response that may be quite different from the structural response computed from a fixed base building subjected to a free field ground motion.

Certainly it is a more simple problem when one can separate the determination of the design ground motion from the dynamic analysis of the building which is the case when one performs a conventional dynamic analysis. This uncoupling of the soil system from the building system may, in general, give a predicted response that could be conservative. For convenience sake, this may be a rationale to use a fixed base model over a soil-structure interaction model. Another reason for this may be that soil-structure interaction involves two distinct disciplines (as practiced in the United States), namely geotechnical and structural engineering. The use of a fixed base model may not be able to take into account all of the possible modes of response such as deformation of the base of the structure or rocking of the structure. Additionally, the periods of vibration of the structure may be longer because of the interaction. In critical structures, such as nuclear reactors, some of these other modes of response may be just as important as the primary translation modes of vibration. The change in period may also affect the response of the overall structure or its substructures or components.

It turns out that in soil-structure interaction analysis, the whole is greater than the sum of the two parts. There needs to be an understanding of both soil dynamics and structural analysis and the ability to combine these two different worlds. Because of the interaction of both the soil and the structure, both need to modeled. However, it should be recognized that, in comparison to the structure, the soil is essentially a semi-infinite medium or unbounded domain. The soil-structure interaction model subjected to dynamic loading cannot be treated in the same way one would consider static loading. When analyzing a soil-structure system under static loading, it is sufficient to model the structure on the soil system which will have fixed or semi-fixed boundaries at a sufficient distance from the structure where these boundary conditions do not affect the static response of the structure. Under dynamic loading, the fictitious boundaries could not be sufficiently far enough away from the structure to not affect the structural response; i.e., the boundaries would reflect the traveling waves within the soil mass and not allow the energy to pass through to infinity. In an attempt to model boundaries properly, special techniques such as the boundary-element method have been developed.

3.8.2 Elements of Soil-Structure Interaction Analysis

Consider two identical structures with a rigid foundation, one founded on stiff rock and the other founded on soft soil, as shown in Figure 3-35. The soil layer overlies the rock and the distance between the two structures is small so that it may be reasonably assumed that the incident earthquake waves arriving from the earthquake source are identical for the two structures. For illustration purposes, we will consider only a vertically propagating shear wave which produces only horizontal motions. A control motion may be defined on the free ground surface of the rock, say at Point A. As the rock is stiff, it may be reasonably assumed that the motion at any point in the rock, say at Point B, is the same as the control motion at Point A.

For the structure founded on the rock, a fixed base condition would exist and the horizontal ground motion applied to the base of the structure by the earthquake would be equal to the control motion. Rocking of the structure would not develop in a fixed base condition.

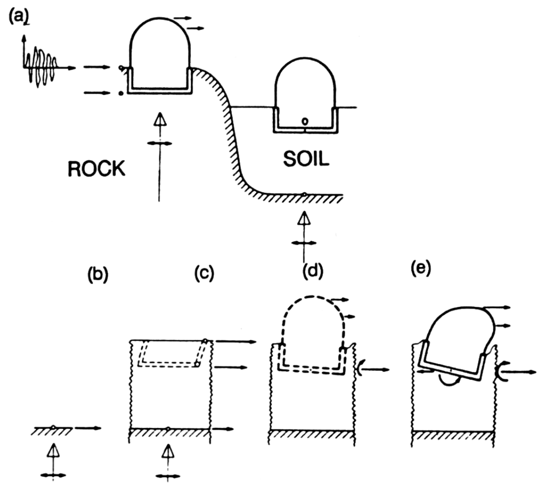

Figure 3-35. Seismic response of structure founded on rock and on soil. (a) sites; (b) outcropping rock; (c) free field; (d) kinematic interaction; (e) inertial interaction

For the structure founded on the soft soil, the earthquake motion at the base of the structure will not be the same as for the structure founded on rock and neither will the base be fixed. The motion at Point C at the top of the rock will not be as great as the motion at Point A because of the presence of the overlying soil layer. As the wave propagates upward in the soil layer, the motion may be amplified or, in some cases, deamplified; in most cases, however, amplification of the motion will occur. The frequency content of the motion will also change. The rigid base of the structure will also modify the motion. The motions will undergo a kinematic interaction which result in the base being subject to some average horizontal displacement and also some rocking. These rigid body motions in the base will apply inertial loading on the superstructure which will excite the structure. The excited structure will then cause a demand on the supporting soils to resist transverse shear and overturning moment. These demands on the soils cause what is referred to as inertial interaction and results in deformations of the soils which ultimately also cause further modification of the motion at the base of the structure.

3.8.3 Limitations of Soil-Structure Interaction Analyses

Implicit in the formulation of present soil-structure interaction analyses is the assumption that the principle of superposition is valid. A result of this assumption is that the response that is computed is for a system that is linear in nature. However, soils are notoriously nonlinear when subjected to strong ground motions at the levels of engineering interest.[3-42] Although it may be possible to use material properties that are compatible with the strain levels produced during an earthquake, this is still far from a true nonlinear analysis.

Because a significant mass of soil must be modeled around the structure, there will be a large number of degrees of freedom which usually impact in computational storage and run time. This may be alleviated by substructuring the problem into two parts. The first part of the analysis is to compute the free field response of the site (without the structure present). The motions are determined at the nodes where the structure is attached. The force-displacement relationships of these nodes are also determined. The second part of the analysis is the study of the superstructure mounted on spring-dashpot systems subjected to the free field motions determined from the first part of the analysis (Fig. 3-36).

Great care must be exercised in soil-structure interaction analyses. The basic assumptions show that, although this type of analysis is more sophisticated than a conventional rigid base analysis, the current state-of-the art still falls far short of modeling reality. Such analyses should be tempered with much engineering judgment. For more detailed information on the theory of soil-structure interaction, the reader is referred to the work by Wolf [3-43].

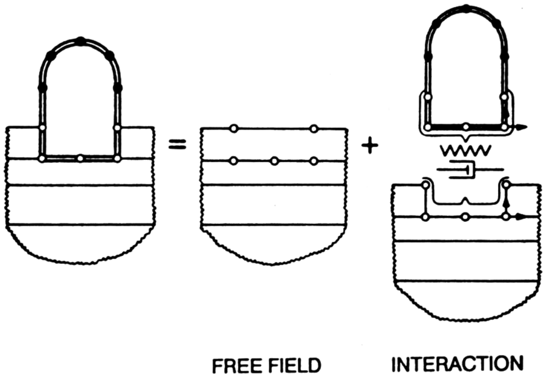

Figure 3-36. Seismic soil-structure interaction with substructure method.

3.9 FAULT RUPTURE

Fault rupture and the associated ground deformation can have extremely severe consequences to structures and systems that cross the fault plane. The fault displacements can range from a few millimeters to several meters. Figure 3-37 shows fault rupture observed in the June 28, 1992 Landers, California earthquake (moment magnitude 7.3) which had maximum horizontal displacements of up to 6 meters across the fault. If ground surface rupture due to earthquake faulting were to occur beneath a structure, there would be substantial damage. Figure 3-38 shows the disruption of a large concrete dam in Taiwan where there was approximately 9 meters of vertical fault offset on the Chelungpu fault in the 1999 Chi-Chi earthquake in Taiwan. Figure 3-39 shows damage to a building caused by faulting, also in Taiwan. The structure would in all likelihood be a substantial, if not a total loss due to the differential ground displacement between the two sides of the fault. This displacement would be mostly lateral if the fault is a strike-slip fault or the displacement would be mostly vertical if the fault is thrust-type fault; some faults will exhibit a combination of these two types of fault movement.

Figure 3-37. Surface fault rupture (up to 6 meters horizontal movement) in the 1992 Landers earthquake.

Figure 3-38. Surface fault rupture beneath reinforced concrete dam in the 1999 Chi-Chi, Taiwan earthquake.

Figure 3-39. Building damaged by faulting during the 1999 Chi-Chi, Taiwan earthquake.

The State of California enacted legislation known as the "Alquist-Priolo Earthquake Fault Zoning Act" in 1972 shortly after the 1971 San Fernando earthquake in which extensive surface faulting damaged numerous homes, businesses and other structures. This act provides the process to mitigate the hazard of surface faulting to structures in California.[3-44] One of the specific criteria given in this legislative act provides that "No structure for human occupancy shall be permitted to be placed across the trace of an active fault." A structure for human occupancy is any structure that has an occupancy rate of 2,000 person-hours per year. For the purposes of the law, an active fault is one that has moved in Holocene time, about the last 11,000 years. The law requires that local jurisdictions must regulate new development projects within these zones determined by the State of California. The local jurisdictions must require a geologic investigation to demonstrate that proposed buildings will not be constructed across active faults. If an active fault is found, a structure for human occupancy cannot be placed over the trace of the fault and must be set back from the fault, usually a distance of at least 50 feet.

The investigation of sites for surface fault rupture hazard may not be simple task. Many active faults are complex and consist of multiple branches that may result in a zone of surface fault rupture. The evidence for identifying active fault traces may be very subtle or obscured. The distinction between recent fault activity and activity that has ceased may be difficult to ascertain. The complexity of evaluation of surface and near-surface faults and the infinite variety of site conditions makes it impossible to use a single investigative method at all sites. Investigation in heavily developed urbanized areas may be extremely difficult.

Fault investigations should first be planned to address the problem of locating existing faults and then attempting to evaluate the recency of the latest fault activity. Data can be obtained from the site and from outside of the site area. Dating of materials may be possible if organic matter is found in the units. The most direct method of evaluating the recency of faulting is to observe, in an open trench or roadway cut, the youngest geologic unit faulted and the oldest geologic unit that is not faulted. Recent active faults may also be identified by direct observation of young, fault-related geomorphic or topographic features in the field, on aerial photographs, or on satellite images. Fault gouge materials may effectively create impermeable barriers that may cause the water level on one side of the fault to be different on the other side. Sometimes evidence of a water barrier (fault) may be seen at the ground surface. Sometimes, the drilling of borings may be needed to determine the differential water levels.

Geophysical methods are indirect methods that require a special knowledge of the geologic conditions for a reliable interpretation. Methods such as seismic refraction, seismic reflection, ground penetrating radar, electrical resistivity, gravity, magnetic intensity can provide useful information, however, they cannot prove the absence of a fault and also cannot determine the recency of activity. These methods should be used very carefully.

3.10 LATERAL SEISMIC EARTH PRESSURES

3.10.1 Active Seismic Earth Pressures

Lateral earth pressures are imposed on retaining structures. Under static conditions, flexible or yielding retaining structures would be subjected to active lateral earth pressures. These active lateral earth pressures are normally computed utilizing the classical theories developed by Coulomb and Rankine. The methodologies to determine the active lateral earth pressures on retaining walls for static conditions may be found in most geotechnical references, such as the United States Navy Design Manual DM-7-02.[3-45]

When there is an earthquake, one can visualize inertial forces from the ground shaking that would impose additional load on a retaining wall. The most commonly used formulation to calculate the seismic lateral earth pressure on a flexible or yielding retaining wall structure is the Mononobe-Okabe formulation which has been described in detail by Seed and Whitman.[3-46] This method is an extension of Coulomb earth pressure theory with the addition of horizontal and vertical forces to account for the earthquake loads. This method assumes that there is sufficient wall movement to produce the minimum wall pressures and that the backfill material consists of dry cohesionless materials. The soil wedge behind the wall is assumed to be at the point of incipient failure and the maximum shear strength is mobilized along the potential sliding surface (see Figure 3-40). The soil mass behind the wall is assumed to behave as a rigid body; therefore, the accelerations are uniform throughout the mass. The effect of the earthquake motions are then represented by inertia forces k_hW and k_vW, where k_hg and k_vg are the horizontal and vertical components of the pseudostatic earthquake accelerations at the base of the wall.

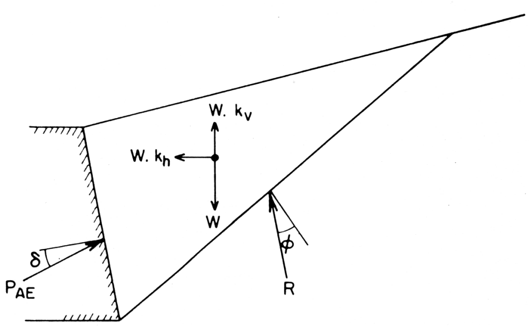

Figure 3-40. Forces acting on an active wedge in Mononobe-Okabe analysis (Ref. 3-46)

The total active thrust is given by an equation that is similar to that developed for static conditions:

$$P_{AE} = (1/2)\,\gamma H^2 (1 - k_v)\, K_{AE}$$

where K_{AE} is the dynamic active earth pressure coefficient which is defined by the following equations:

$$K_{AE} = \frac{\Im}{\Re\left[1+\sqrt{\dfrac{\sin(\phi+\delta)\sin(\phi-\theta-i)}{\cos(\delta+\beta+\theta)\cos(i-\beta)}}\right]^2}$$

where

$\Im = \cos^2(\phi-\theta-\beta)$ and

$\Re = \cos\theta\cos^2\beta\cos(\delta+\beta+\theta)$

θ = $\tan^{-1}[k_h/(1-k_v)]$
γ = moist unit weight of the soil
H = height of wall
ϕ = angle of internal friction of the soil
δ = angle of wall friction
i = angle of ground surface slope behind the wall
β = angle of slope of back of wall to vertical
k_h = pseudostatic horizontal ground acceleration/g
k_v = pseudostatic vertical ground acceleration/g

The horizontal component of the force P_{AE} may be expressed as P_{AEh}, where

$$P_{AEh} = P_{AE}\cos(\delta+\beta) = (1/2)\,\gamma H^2 (1 - k_v)\, K_{AE}\cos(\delta+\beta)$$

For a wall with a vertical inside face ($\beta = 0$):

$$P_{AEh} = (1/2)\,\gamma H^2 (1 - k_v)\, K_{AE}\cos\delta$$

It should be remembered that the computed lateral force includes the static lateral active earth pressure and the dynamic increment of earth pressure which can be expressed as:

$$P_{AE} = P_A + \Delta P_{AE}$$

The static component, P_A, acts at a height of H/3 above the base of the wall. For cantilevered retaining structures, most investigators have agreed that the point of application of the resultant of the dynamic earth pressure should be at a height of 0.5H to 0.67H above the base of the wall [3-46]. Prakash has recommended that the point of application of the resultant be taken at 0.55H above the base of a flexible wall and at 0.45H above the base of a rigid wall.[3-47] Seed and Whitman recommended that the dynamic component be assumed to act at about 0.6H above the base of the wall.

The selection of the pseudostatic accelerations is a critical matter. If one uses anticipated peak ground accelerations, the computed lateral thrust may be very unrealistically high. As this method uses pseudostatic accelerations very much like slope stability analyses, values of the horizontal acceleration, k_h, between 0.05g and 0.15g, are commonly used, according to Whitman [3-48]; these values may correspond to one-third to one-half of the peak ground accelerations. Elms and Martin [3-49] have suggested that the horizontal acceleration, k_h, be taken as one-half of the peak ground acceleration (0.5A), provided that there be an allowance for an outward displacement of 10 A inches or 250 A millimeters. The vertical acceleration, k_v, may be taken as one-half to two-thirds of k_h.

There are other methods of analyses for seismic active earth pressures on walls. Some of these methodologies are discussed in Kramer.[3-50]

3.10.2 Passive Seismic Earth Pressures

As seismic activity can cause the active earth pressures to increase dramatically due to ground shaking, the same earthquake influences can cause the passive resistance of the soil to decrease. Mononobe and Okabe also formulated a theory for the seismic passive resistance of soils against a wall.

The equation for the total passive thrust on a wall retaining a dry, cohesionless backfill is given in the following equation:

$$P_{PE} = (1/2)\,\gamma\,H^2\,(1 - k_v)\,K_{PE}$$

where the dynamic passive earth pressure coefficient, K_{PE}, is given by the following:

$$K_{PE} = \frac{\Im}{\Re\left[1 - \left\{\dfrac{\sin(\phi-\delta)\sin(\phi+i-\theta)}{\cos(i-\beta)\cos(\delta-\beta+\theta)}\right\}^{1/2}\right]^2}$$

where

$\Im = \cos^2(\phi-\theta-\beta)$ and

$\Re = \cos\theta\cos^2\beta\cos(\delta-\beta+\theta)$

The total passive thrust can also be separated into its static and dynamic components as follows:

$$P_{PE} = P_P + \Delta P_{PE}$$

It should be noted that P_{PE} will be less than P_P as the dynamic component, ΔP_{PE}, acts in an opposite direction from the static component. In other words, the Mononobe-Okabe equation predicts that the available passive resistance will be reduced during earthquake ground shaking.

3.11 CONCLUSIONS

It has been shown that the earthquake ground motions that affect structures are greatly influenced by the local site and geologic conditions. It has also been demonstrated that the ground motion response may also be influenced more greatly at different structural periods of vibration. These effects have been recognized and have been incorporated into the latest United States building codes as discussed in this chapter. Recognition of near-source effects has also been incorporated into the building codes.

Soil liquefaction is a major concern in seismically active areas that have young geologic materials with a shallow groundwater condition. Various methods of analysis have been presented that use different in-situ soil characterization technologies. The consequences of liquefaction also need to be evaluated to determine the effects on structures founded in such conditions. Methods of analysis to evaluate liquefaction-induced settlement and lateral spreading have been presented. Also presented is a discussion of the most commonly used techniques to mitigate the effects of liquefaction to allow for engineered construction to proceed.

A discussion of other geologic-seismic hazards has also been presented. These hazards include seismic settlement, fault rupture, landsliding, tsunamis, and lateral seismic pressures on buried structures. The practice of geotechnical earthquake engineering is still evolving and further advances are expected to appear on the horizon in short order. It is expected that many of the existing technologies will be unproved or replaced with more advanced methods in the future.

REFERENCES

3-1. International Conference of Building Officials, *Uniform Building Code*, 1976 Edition, Whittier, California.

3-2. International Conference of Building Officials, *Uniform Building Code*, 1985 Edition, Whittier, California.

3-3. International Conference of Building Officials, *Uniform Building Code*, 1988 Edition, Whittier, California.

3-4. International Conference of Building Officials, *Uniform Building Code*, 1994 Edition, Whittier, California.

3-5. International Conference of Building Officials, *Uniform Building Code*, 1997 Edition, Whittier, California.

3-6. Seismology Committee, Structural Engineers Association of California, *Recommended Lateral Force Requirements and Commentary,* Sixth Edition, Sacramento, California, 1996.

3-7. Federal Emergency management agency, NEHRP Recommended provisions for Seismic Regulations for New Buildings and Other Structures, 1997 Edition, FEMA302, Washington, D.C.

3-8. International Conference of Building Officials, *Maps of Known Active Fault Nearing Source Zones in California and Adjacent Portions of Nevada,* Whittier, California, 1988.

3-9. Lew, Marshall and Bonneville, David, *New Building Code Requirements for the Seismic Design of Tall Buildings Near Active Faults,* Proceedings, Fourth Conference on Tall Buildings in Seismic Regions, Los Angeles, California, 1997.

3-10. International Code Council, *International Building Code,*2000 Edition.

3-11. Seed, H.B., Tokimatsu, K., Harder, L.F., and Chung, R.M., *The Influence of SPT Procedures in Soil Liquefaction Resistance Evaluations*, University of California Berkeley, Report No. UCB/EERC-84-15, October 1984.

3-12. Youd, T.L. and Idriss, I.M., *Proceedings of the NCEER Workshop on Evaluation of Liquefaction Resistance of Soils,* National Center for Earthquake Engineering Research, Technical Report NCEER-97-0022, 1997.

3-13. Seed, H.B., Idriss, I.M., and Arango, I., "Evaluation of Liquefaction Potential Using Field Performance Data," Journal of the Geotechnical Division, ASCE, Vol. 109, No. 3, March 1983.

3-14. Seed, H.B., and Idriss, I.M., "Ground Motions and Soil Liquefaction During Earthquakes," Earthquake Engineering Research Institute, Berkeley, California, 1982.

3-15. Ishihara, K. And Yoshimine, M., *Evaluation of Settlements in Sand Deposits Following Liquefaction During Earthquakes*, Soils and Foundations, Japanese Society of Soil Mechanics and Foundation Engineering, Vol. 32, No. 1, March 1992.

3-16. Youd, L.T., "Major Cause of Earthquake Damage is Ground Failure," Civil Engineering, Vol. 48, No. 4, pp. 47-51, April, 1978.

3-17. Youd, L.T., "Ground Failure Displacement and Earthquake Damage to Buildings," Proceedings, 2nd ASCE Conference on Civil Engineering and Nuclear Power, Knoxville, Tennessee, September, 1980.

3-18. Ishihara, K., "Stability of Natural Deposites During Earthquakes," Proceedings of the 11th International Conference on Soil Mechanics and Foundation Engineering, San Francisco, 1985.

3-19. Youd, L.T., and Garris, C.T., "Liquefaction-Induced Ground Surface Disruption," Fifth United States-Japan Workshop on Earthquake Resistant Design of Lifeline Facilities and Countermeasures Against Liquefaction, National Center for Earthquake Engineering Research Technical Report, Tokyo, Japan, 1994

3-20. Prevost, J.H., "DYNA-FLOW: A Nonlinear Transient Finite Element Analysis Program," Report No. 81-SM-1, Department of Civil Engineering, Princeton University, Princeton, N.J., 1981.

3-21. Finn, W.E.L. and Yogendrakumar, M., "TARA-3FL: Program for Analysis of Liquefacion Induced Flow Deformations," Department of Civil Engineering, University of British Columbia, Vancouver, B.C., Canada, 1989.

3-22. Newmark, N.M., "Effects of Earthquakes on Dams and Embankments," Geotechnique, Vol. 15, No. 2, 1965.

3-23. Byrne, P.M., Jitno, H., and Salgado, F., "Earthquake Induced Displacement of Soil-Structures Systems," Proceedings, 10th World Conference on Earthquake Engineering, Madrid, Spain, 1992.

3-24. Bartlett, S.F. and Youd, T.L., "Empirical Analysis of Horizontal Ground Displacement Generated by Liquefaction-Induced Lateral Spread," National Center for Earthquake Engineering Research, Technical Report NCEER-92-0021, 1992.

3-25. National Research Council, "Liquefaction of Soils During Earthquakes," National Academy Press, Washington, D.C., 1985.

3-26. Hayden, R.F., "Utilization of Liquefaction Countermeasures in North America," Fifth U.S. National Conference on Earthquake Engineering, Earthquake Engineering Research Institute, Chicago, July 1994.

3-27. Hayden, R.F. and Baez, J.I., "State of Practice for Liquefaction Mitigation in North America," Fifth United States-Japan Workshop on Earthquake Resistant Design of Lifeline Facilities and Countermeasures Against Liquefaction, National Center for Earthquake Engineering Research Technical Report, Tokyo, Japan, 1994

3-28. Brown, R.E., "Vibroflotation Compaction of Cohesionless Soils," Journal of Geotechnical Division, ASCE, Vol. 103, No. GT12, pp. 1437-1451, December, 1977.

3-29. Ishihara, K., Iwasake, Y., and Nakajima, M., "Liquefaction Characteristics of Sand Deposits at an Oil Tank Site During the 1978 Miyagiken-Oki Earthquake," Soil and Foundations, Vol. 20, No. 2, pp. 97-111, June, 1980.

3-30. Slocombe, B.C., "Dynamic Compaction," Chapter 2 in *Ground Improvement*, M.P. Moseley (ed.), Blackie Academic & Professional, Bishopbriggs, Glasgow, 1993.

3-31. Taki, O. and Yang, D.S., "Soil-Cement Mixed Wall Technique," ASCE, Geotechnical Engineering Congress, Boulder, Colorado, 1991.

3-32. Pujol-Rius, A., Griffin, P., Neal, J., and Taki, O., "Foundation Stabilization of Jackson Lake Dam," 12th International Conference on Soil Mechanics and Foundation Engineering, Brazil, 1989.

3-33. Babasaki, R., Suzuki, K., Saitoh, S., Suzuki, Y., and Tokitoh, K., "Construction and Testing of Deep Foundation Improvement Using the Deep Cement Mixing Method," in *Deep Foundation Improvments: Design, Construction, and Testing*, ASTM STP 1089, Philadelphia, 1991.

3-34. Hunt, R.E., "Geotechnical Engineering Investigation Manual," McGraw-Hill Book Company, New York, 1984.

3-35. Whitman, R.V., and DePablo, P.O., "Densification of Sand by Vertical Vibrations," Proceedings, 4th World Conference on Earthquake Engineering, Santiago, Chile, 1980.

3-36. Lambe, W.T., and Whitman, R.V., "Soil Dynamics," John Wiley & Sons, New York, 1969.

3-37. Tokimatsu, K. and Seed, H.B., "Evaluation of Settlements in Sands due to Earthquake Shaking," Journal of Geotechnical Engineering, ASCE, Vol. 113, No. 8, August 1987.

3-38. Seed, H.B. and Idriss, I.M., "Simplified Procedure for Evaluating Soil Liquefaction Potential," Journal of the Soil Mechanics and Foundations Division, ASCE, Vol. 97, No. SM9, 1971.

3-39. Seed, H.B., and Wilson, S.D., "The Turnagain Heights Landslide, Anchorage, Alaska," Journal of the Soil Mechanics and Foundation Engineering Division, ASCE, Vol. 93, No. SM4, pp. 325-353, July, 1967.

3-40. Legget, R.F., and Karrow, P.F., "Handbook of Geology in Civil Engineering," McGraw-Hill Book Company, New York, 1983.

3-41. Wiegel, R.E. (editor), "Earthquake Engineering," Prentice Hall, Englewood Cliffs, New Jersey, 1970.

3-42. Seed, H. B., "Earthquake Effects on Soil-Foundation Systems," in Foundation Engineering Handbook, H.F. Winterkorn and H.Y. Fang (editors), Van Nostrand Reinhold Company, New York, 1975.

3-43. Wolf, J.P., "Dynamic Soil-Structure Interaction," Prentice Hall, Englewood Cliffs, New Jersey, 1985.

3-44. Hart, E.W., "Fault-rupture hazard zones in California," California Department of Conservation, Division of Mines and Geology, Special Publication 42, Revised 1994.

3-45. Naval Facilities Engineering Command, *Foundations & Earth Structures*, Design Manual 7.02, Alexandria, Virginia, 1986.

3-46. Seed, H.B., and Whitman, R.V., "Design of Earth Retaining Structures for Dynamic Loads," Proceedings of ASCE Specialty Conference on Lateral Stresses in the Ground and Design of Earth Retaining Structures, Ithaca, New York, pp 103-147, 1970.

3-47. Prakash, S., "Soil Dynamics," McGraw-Hill Book Company, New York, 1981.

3-48. Whitman, R.V., "Seismic design behavior of gravity retaining walls," Proceedings, ASCE Specialty Conference on Design and Performance of Earth Retaining Structures, Geotechnical Specialty Publication 25, ASCE, New York, 1990.

3-49. Elms, D.G, and Martin, G.R., *Factors Involved in the Seismic Design of Bridge Abutments,* Applied Technology Council Workshop on Earthquake Resistance of Highway Bridges, ATC-6-1, 1979.

3-50. Kramer, Steven L., *Geotechnical Earthquake Engineering*, Prentice Hall, Inc., 1996.